Hindawi
Journal of Chemistry
Volume 2023, Article ID 9807940, 1 page
https://doi.org/10.1155/2023/9807940

Retraction

Retracted: Design of Noise-Reducing Two-Stage Cage Control Valve and Its Fluid Characteristics and Cavitation Study

Journal of Chemistry

Received 28 November 2023; Accepted 28 November 2023; Published 29 November 2023

This article has been retracted by Hindawi, as publisher, following an investigation undertaken by the publisher [1]. This investigation has uncovered evidence of systematic manipulation of the publication and peer-review process. We cannot, therefore, vouch for the reliability or integrity of this article.

Please note that this notice is intended solely to alert readers that the peer-review process of this article has been compromised.

Wiley and Hindawi regret that the usual quality checks did not identify these issues before publication and have since put additional measures in place to safeguard research integrity.

We wish to credit our Research Integrity and Research Publishing teams and anonymous and named external researchers and research integrity experts for contributing to this investigation.

The corresponding author, as the representative of all authors, has been given the opportunity to register their agreement or disagreement to this retraction. We have kept a record of any response received.

References

[1] R. Yu and X. Lu, "Design of Noise-Reducing Two-Stage Cage Control Valve and Its Fluid Characteristics and Cavitation Study," *Journal of Chemistry*, vol. 2022, Article ID 7322655, 23 pages, 2022.

Hindawi
Journal of Chemistry
Volume 2022, Article ID 7322655, 23 pages
https://doi.org/10.1155/2022/7322655

Research Article

Design of Noise-Reducing Two-Stage Cage Control Valve and Its Fluid Characteristics and Cavitation Study

Ruiming Yu and Xi Lu

School of Mechanical Engineering, University of Shanghai for Science and Technology, Shanghai 200093, China

Correspondence should be addressed to Ruiming Yu; 211170097@st.usst.edu.cn

Received 21 July 2022; Revised 27 August 2022; Accepted 30 August 2022; Published 23 September 2022

Academic Editor: Rabia Rehman

For all kinds of media noise, noise reduction valve cage cannot meet the equal percentage flow characteristics, and for manufacturing and processing and other technical problems, research and design of new noise reduction two-stage cage control valve are necessary. The valve adopts noise reduction valve cage and curve valve cage with noise reduction, forming a two-stage noise reduction, with uniform flow, diffusion, and noise reduction effect, to meet the regulating valve equal percentage flow characteristics. The spool is evenly stressed and not easy to loosen and fall off, and the small opening is not easy to vibrate and shake. The flow characteristics of the noise-reducing two-stage cage control valve are studied, and the fluid flow coefficients, flow characteristic curves, the relationship of flow coefficients with nominal diameter at the same stroke, and the relationship of flow coefficients with different nominal diameters at different strokes are analyzed. The relationship between nominal diameter constant opening and cavitation coefficient with inlet velocity, the relationship between inlet velocity and cavitation coefficient with nominal diameter at half opening, and the relationship between inlet velocity and cavitation coefficient with nominal diameter at full opening were studied, and the cavitation generation and its effect on noise were analyzed. The noise and cavitation test showed that noise is very small and cavitation is difficult to produce, all meeting the noise reduction requirements.

1. Introduction

In petroleum, petrochemical, power plant, refining, chemical, and pharmaceutical industries, it is often necessary to regulate and control the flow, pressure, and temperature of steam, gas-liquid two-phase flow, gas, and other media [1, 2] to meet the needs of various chemical reactions or heating and cooling transduction [3, 4]. This has been studied by many scholars. By using high pressure as a processing tool, high-pressure technologies using subcritical and supercritical fluids offer the possibility to obtain new products with special characteristics or to design new processes that are environmentally friendly and sustainable [5]. Supercritical fluids have been used in several processes developed to commercial scale in the pharmaceutical, food, and textile industries. Bao et al. [6] utilized a unique microscale phenomenon of microfluidic systems to provide fast, accurate, and robust analysis, primarily for biomedical, oil, and gas applications. In addition to obtaining high temperatures and pressures, it has also driven extended applications in phase measurements associated with industrial carbon monoxide. Tan et al. [7] studied that as an important reactor form for catalytic reactions of gases, liquids, and solids, and the trickle-bed reactor (TBR) is widely used in the petroleum, biochemical, fine chemical, and pharmaceutical industries due to its flexibility, operational simplicity, and high throughput. Reactors are subject to high temperatures and pressures, fluid flow rates, and flow rates that need to be controlled during catalytic reactions. Ballesteros Martínez et al. [8] analyzed the low fluid load flows that often occur during the transport of gas products in various industries, such as oil and gas, food, and pharmaceutical industries. Modeling low liquid load flow rates in medium-sized (6–10 inches) pipelines analyzed how the presence of the liquid phase has a greater effect on process variables than its exact flow rate. Introducing the liquid phase into a single-phase

gas results in a threefold increase in pressure loss, but doubling the liquid velocity only increases the pressure loss by a further 30%.

Although the pressure before the valve or the pressure difference before and after the valve is only 0.4 MPa~2 MPa, the inherent noise characteristics of gas, liquid, and gas-liquid two-phase media can produce noise that affects the environment and human physiology when the opening degree changes [9–11]. Many papers [12–16] have analyzed and studied the valve noise with some results. For the cavitation and noise problems of hydraulic tapered valves, the variation laws of cavitation and noise are obtained based on the spool radial force analysis and considering the radial deviation of the spool [17]. The cavitation intensity changes slowly with the half cone angle of 45° and the noise level is minimized. Properly increasing the opening within a reasonable range can effectively suppress cavitation and reduce the noise level [18]. The effect of pressure and flow rate of conical throttle valve on cavitation noise is studied. The larger the pressure difference before and after the valve is, the more obvious cavitation is and the stronger the cavitation noise is, and the cavitation noise can be suppressed by reducing the pressure difference before and after the valve. Li et al. [19] proposed a numerical simulation method that integrates dipole and quadrupole sources to predict the aerodynamic noise during safety valve venting. The simulation method is used to calculate the exhaust noise of safety valve under six different working conditions and analyze the sound source characteristics of safety valve exhaust noise. Wei et al. [20] studied the characteristics of flow-induced noise in a high-pressure pressure reducing valve, based on computational fluid dynamics, using a numerical method to calculate the flow field and applying the Ffowcs Williams and Hawkings model to obtain the acoustic signal. Numerous scholars have studied the noise generation mechanism, influencing factors, and change patterns.

A frequently used noise reduction method is the installation of a noise reduction valve cage with holes drilled in the cage, which can only satisfy the linear flow characteristics due to the uniform distribution of the holes [21, 22]. Sotoodeh [23] investigated valve cages with many small holes drilled in the control valve to divide the flow into many small flows, using this design to reduce noise. Kang et al. [24] drilled many small holes in the valve cage according to the small outlet flow rate to meet the low noise requirement. Lah [25] analyzed that noise sounds more like a small explosion in a valve and the cage is either slotted or drilled to control the location in the valve where cavitation occurs and reduce the noise. If the equal percentage flow characteristics are to be satisfied, the holes must be drilled unevenly within 50% of the opening and the diameters of the holes must also be unevenly distributed, which will dramatically increase the manufacturing cost and processing difficulty by several times [26], and the use of the results is not satisfactory. Therefore, there is a need to research and design a regulating valve that can reduce noise, meet the equal percentage flow characteristics, and be easy to manufacture and process.

For all kinds of media noise, noise reduction valve cage cannot meet the equal percentage flow characteristics, and for manufacturing and processing and other technical problems, research and design of new noise reduction two-stage cage control valve are necessary. The cage type control valve can effectively reduce the harmful noise generated by gas, steam, and gas-liquid medium and can perfectly ensure the equal percentage flow characteristics of the control valve, making the process parameter (flow, pressure, temperature, etc.) adjustment quality excellent, widely used in steam, gas-liquid two-phase flow, gas, evacuation, and other noise overload conditions, for the regulation and control of process parameters.

2. Materials and Structure

2.1. Materials. Each component of the control valve is made of low-temperature carbon steel LCB, alloy steel casting WC6, pressure casting austenitic CF8M, stainless steel 304 and 316, martensitic stainless steel 420, etc. The material of each main component is shown in Table 1.

LCB is a kind of low-temperature carbon steel of American standard, which is a grade of cast steel, and 20# is a high-quality carbon structural steel of national standard. It is a low alloy steel with a temperature range of −46~343 and is generally used to manufacture valves. CF8M belongs to stainless steel. CF8M is an American stainless steel grade, which is equivalent to 316 stainless steel in our country. The maximum carbon content of this type of stainless steel is 0.08%, and it contains molybdenum elements. Its tensile strength is 485 MPa, and it has good corrosion resistance, good welding performance, and plasticity. It has the advantages of high strength and high temperature resistance and is used to make valve castings and chemical equipment. Among the components of stainless steel, 304 and 316 are the most used ones; they can be used as the inner liner of the thermos cup and can be made into various cookware and instruments. It is also a food-grade material, which is safe enough to be used in daily life. 304 stainless steel contains about 18% chromium and more than 8% nickel; on this basis, 316 stainless steel also adds 2% molybdenum, which has better corrosion resistance. There are also 201 series stainless steel and 430 series stainless steel. Compared with the above two, their quality and advantages are much weaker, so the usage rate is not high. Because 316 stainless steel contains molybdenum element, its anti-corrosion effect is better, and the performance of acid and alkali resistance is also improved. 304 stainless steel lacks molybdenum, so its corrosion resistance and acid and alkali resistance are not as good as 316. Although both are food-grade materials, they are used in different fields. For example, 316 stainless steel has good corrosion resistance, and many medical devices are made of 316.304 stainless steel is widely used in cookware, tableware, etc. and has a wide range of uses. Stainless steel countertops, cooking pots, and stainless steel tableware in our home all use 304.

2.2. Structure. Noise-reducing two-stage cage control valve structure includes valve body, valve seat, valve spool, noise-reducing cage, curved cage, valve stem, valve cover, packing,

Table 1: Each main component material.

Names	Valve seat	Valve body	Valve stem	Valve cover	Valve spool
Materials	316	LCB	420	WC6	CF8M

gland, disc spring, pressure plate, ball valve, clearance, long neck large window, short neck small window, and long neck area, and the structure is shown in Figure 1.

3. Design Method

The noise reduction double-stage cage adjustment valve includes valve body, valve seat, valve cover, valve stem, and valve spool. The packing is automatically compensated by the gland, disc spring, and pressure plate cooperatively pressed on the bonnet. The valve stem is connected to the valve spool, the valve seat is set in the valve body, the valve spool is sealed with the valve seat in contact, the valve body is provided with a noise reduction cage, the noise reduction cage is provided with noise reduction holes, the noise reduction cage is also provided with a curved valve cage, the curved valve cage is provided with a flow window, the valve spool is set in the curved valve cage axial movement, the valve spool and the curved valve cage cooperate to control the flow window opening size, and the noise reduction cage and the curved valve cage form a valve cage structure located above the valve seat through the valve spool in the curved valve cage to change the flow window opening size, so as to control the flow.

The noise reduction holes on the noise reduction valve cage are evenly distributed on the noise reduction valve cage and staggered up and down, and the noise reduction holes are set up with uniform flow rate and good diffusion effect, which can effectively reduce noise. The noise-reducing valve cage material adopts stainless steel nitriding treatment to improve the scouring resistance of the noise-reducing holes on the cage and the overall pressure-bearing strength of the cage. The diameter of the noise reduction hole is set from Φ1 mm to Φ6 mm, and the noise reduction valve cage adopts the internal and external double-layer valve cage structure, with a gap between the internal and external double-layer valve cage structure, and the noise reduction effect is better.

The flow window on the curve valve cage includes long-necked large window and short-necked small window, the long-necked large window and short-necked small window are the same and evenly distributed in a circle on the curve valve cage, making the number of flow windows on the curve valve cage increased and evenly distributed, the fluid beam distribution is more uniform, the flow window can not only control the flow volume but also achieve the purpose of noise reduction. It is similar to the noise reduction valve cage in forming a two-stage noise reduction function; with the increase of the number of flow windows on the curve cage, the rotating torque around the valve core is evenly distributed, eliminating the looseness and falling off problems caused by uneven force on the valve core. The number of flow windows on the curve cage is 8~16 and even, and they can be set symmetrically. The long neck area of the long neck window is biased towards the valve seat, as shown in Figure 2, the long neck area exceeds the short neck small window biased towards the valve seat, the long neck large window and the short neck small window cooperate to form a flow window with equal percentage flow characteristics, and the flow window is made according to the equal percentage flow characteristics; the flow window on the curve valve cage is used to achieve noise reduction and at the same time can meet the equal percentage flow characteristic adjustment. When the long-necked large window is in small opening, the spool only needs to open the long-necked area of the long-necked large window for small opening flow control, and in small opening, the area where the spool opens the flow window is concentrated in the long-necked area of the long-necked large window, in the case of uniform distribution of the long-necked large window and short-necked small window, avoiding the problems of small opening, and when the flow window size is too small, flow resistance is too large, flow rate is too fast, and flow rate instability causes valve vibration and oscillation.

Noise reduction valve cage and curve valve cage have a gap between them so that the media can be redistributed after passing through the upper cage and the media can flow evenly into the next cage, balancing media energy.

4. Fluid Properties

4.1. Fluid Flow Coefficient. By keeping the differential pressure flow coefficient between the inlet and outlet of the regulating valve at 105.5, the water flow rate of 40 ° C per hour can be obtained, which can measure the flow capacity of the regulating valve and facilitate the research on the opening and closing, regulation, noise reduction, and other performances of the regulating valve. A larger value of the flow coefficient (Cv) indicates a better flow capacity of the regulating valve. For incompressible fluids [27],

$$C_v = \frac{10U}{\sqrt{\Delta p/\varepsilon}}, \tag{1}$$

where C_v is the flow coefficient, U is the volume flow, Δp is the differential pressure before and after the control valve, and ε is the relative density of water which is 1.

For compressible media, such as gases, the compressible gas flow coefficient based on the expansion coefficient method is used. Control valve differential pressure ratio K is less than the product of the critical differential pressure ratio K_t and specific heat ratio coefficient λ ($K < K_t\lambda$), and the flow inside the valve cavity is non-blocking flow:

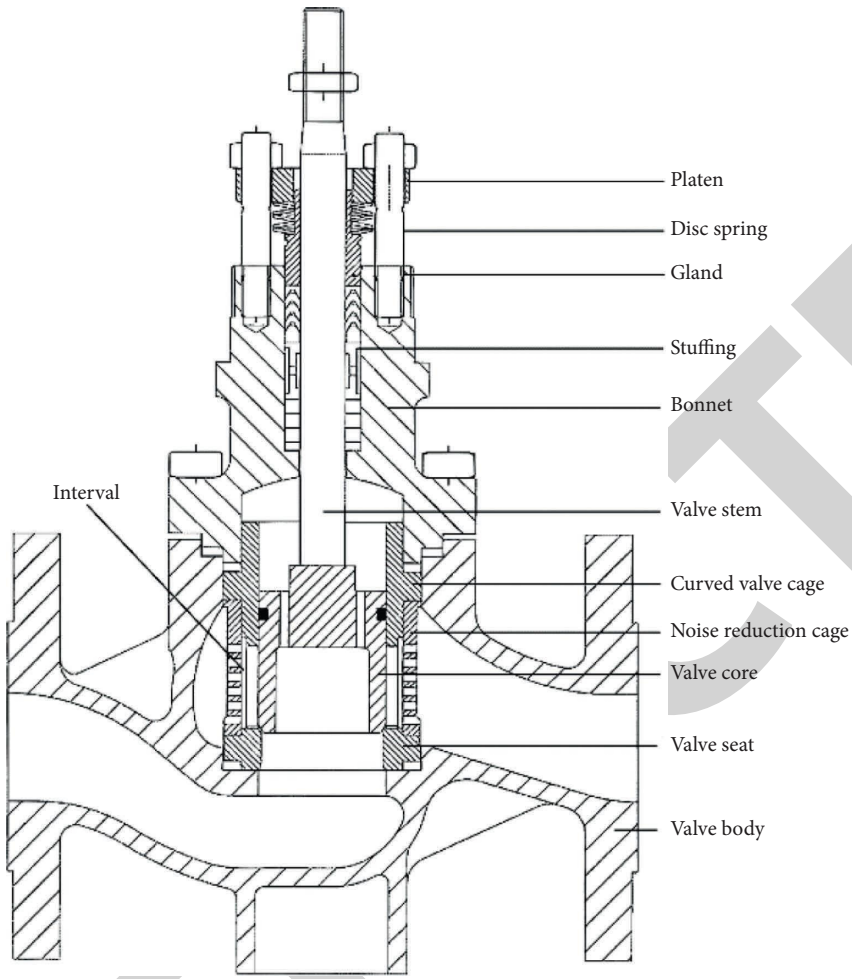

Figure 1: Noise-reducing two-stage cage control valve structure.

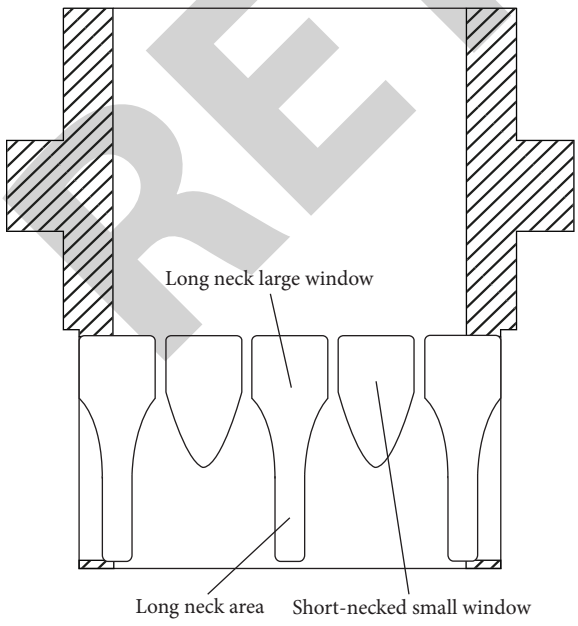

Figure 2: Curved valve cage structure.

$$C_v = \frac{U_0}{4.44 p_1 \eta}\sqrt{\frac{T\rho_1 Y}{K}},$$
$$\eta = 1 - \frac{K}{3\lambda K_t}, \quad (2)$$
$$K = \frac{\Delta p}{p_1},$$

where U_0 is the gas standard volume flow rate, p_1 is the prevalve pressure, η is the gas flow through the regulating valve density change expansion coefficient, T is the control valve inlet temperature, ρ_1 is the gas density at 273.15 K, 101300 Pa, Y is the compression factor, K is the compression ratio, K_t is the critical pressure difference ratio, and λ is the specific heat ratio coefficient.

Control valve differential pressure ratio$K$is greater than or equal to the product of the critical differential pressure ratio$K_t$and specific heat ratio coefficient λ ($K \geq K_t\lambda$), the internal flow of the valve cavity for blockage flow. The pressure before the valve$p_1$remains constant, and gradually reduce the pressure after the valve; the flow will not increase, at this time,

$$C_v = \frac{U_0}{2.48 p_1} \sqrt{\frac{T_0 \rho_1 Y}{\varsigma K_t}}, \quad (3)$$

where T_0 is the regulating valve inlet temperature during blockage flow and ζ is the gas isentropic index.

4.2. Flow Rate Characteristic Curve. Cv of each opening of the noise-reducing two-stage cage control valve is measured through the flow test. The characteristic test system of the control valve flow test system includes pressure pump, thermometer, throttle valve, temperature sensor, flow sensor, pressure sensor and flow meter, and so on. The schematic diagram of the control valve flow test system is shown in Figure 3.

The pipe before and after the control valve is a straight section, the length of the straight section needs to meet the test requirements to ensure that the fluid flow rate is uniform and continuous, and the nominal size of the test pipe and the location of the control valve are shown in Figure 4.

The pressure difference Δp, Cv, pressure recovery coefficient FL, flow resistance coefficient μ, and temperature t are measured for each degree of opening from 0% to 100% and from fully closed to fully open at 5% intervals, taking into account the flow status, piping material, and application conditions. The test medium is room temperature water at 21.6°C with a density of 1 g/cm^3. Fluid flow through the regulating valve produces flow resistance consumption and the pressure recovery coefficient FL:

$$\mathrm{FL} = \frac{U_{\max}}{0.1 C v \sqrt{(p_1 - 0.96 p_e)/p}}, \quad (4)$$

where FL is the pressure recovery factor, $U_{\max}$ is the maximum volume flow rate, p_e is the fluid saturated vapor pressure at the inlet temperature of the control valve, and ρ is the fluid density.

Fluid flow resistance coefficient [28]:

$$\mu = \frac{2\Delta p}{\rho v^2}, \quad (5)$$

where μ is the flow resistance coefficient and v is the flow rate.

Nominal diameter DN65, stroke of $L = 50$ mm, adjustable ratio of 50, rated Cv value of 85. differential pressure Δp, Cv, pressure recovery coefficient FL, flow resistance coefficient μ, and temperature t at each opening of the control valve are shown in Table 2.

The flow characteristic curve of the regulating valve is shown in Figure 5 by fitting the curve to the Cv value at each opening degree.

As seen in Figure 5, the flow characteristic curve of the noise-reducing two-stage cage control valve refers to equal percentage flow characteristic, indicating that the long-necked flow large window and short-necked flow small window on the curved valve cage ensure the equal percentage flow characteristic of the control valve. At 50% opening, the Cv value is 12.02, and at 100% opening, the Cv value is 85. At 0% to 50% opening, the Cv increases slowly and the flow is slow, and at 50% to 100% opening, the Cv increases dramatically and the flow capacity rises. The control valve regulates the flow smoothly and accurately and can meet the requirements of various media and working conditions.

The Cv curves for the nominal diameters DN65, DN80, and DN100 of the regulating valve with stroke $L = 50$ mm are shown in Figure 6.

For the same stroke $L = 50$ mm, the rated Cv is 85 for nominal diameter DN65, 110 for DN80, and 200 for DN100. From DN65 to DN80, the Cv increases by 25 for a 15 mm increase in nominal diameter and by 90 for a 20 mm increase in nominal diameter from DN80 to DN100. Under the same stroke, increasing the nominal diameter can improve the flow capacity of the regulating valve and nominal diameter with a small increase; the rated Cv will increase significantly, the flow capacity will also increase significantly, and the smaller the pressure loss of fluid through the regulating valve, the better the noise reduction of two-stage cage regulating valve flow regulation performance.

Itinerary $L = 50$ mm, nominal diameter DN80, stroke $L = 60$ mm, nominal diameter DN125, stroke $L = 75$ mm, nominal diameter DN200, stroke $L = 100$ mm, nominal diameter 300, stroke $L = 150$ mm, nominal diameter DN400, different strokes, different nominal diameters, and Cv curves are shown in Figure 7.

For different strokes and different nominal diameters, the rated Cv for stroke $L = 60$ mm, nominal diameter DN125 is 280, stroke $L = 75$ mm, nominal diameter DN200 is 690, stroke $L = 100$ mm, nominal diameter DN300 is 1300, stroke $L = 150$ mm, and nominal diameter DN400 has a rated Cv which is 1800; from DN80 to DN125, the nominal diameter increases by 45 mm, and the Cv increases by 170; from DN125 to DN200, the nominal diameter increases by 75 mm, and the Cv increases by 410; from DN200 to DN300, the nominal diameter increases by 100 mm, and the Cv increases by 610; from DN300 to DN400, the nominal diameter increases by 100 mm and the Cv increases by 500, indicating that the increase is stepwise; as the stroke increases, the nominal diameter also increases gradually, the rated Cv increases, and the curvature of the Cv curve increases rapidly, all of which are equal percentage characteristics. If the stroke increases, the nominal diameter increases; with the increase of opening, the Cv increases; if the same opening stroke and nominal diameter are large, the flow coefficient is also large, and the regulating valve flow capacity increases. For noise reduction double-stage cage adjustment for different strokes and different nominal diameters, the flow characteristics are equal percentage flow characteristics, and flow adjustment is gentle and sensitive.

4.3. Fluid Dynamics Simulation Analysis. Noise-reducing two-stage cage control valve with nominal diameter DN65 and rated stroke of $L = 50$ mm (Solidworks modeling) is shown in Figure 8.

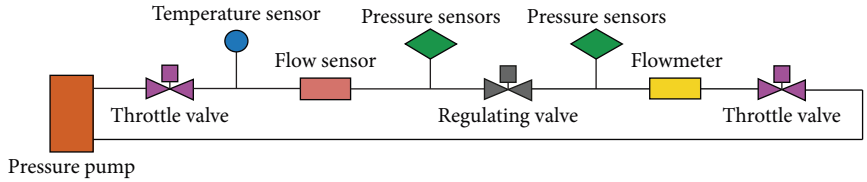

Figure 3: Schematic diagram of the control valve flow test system.

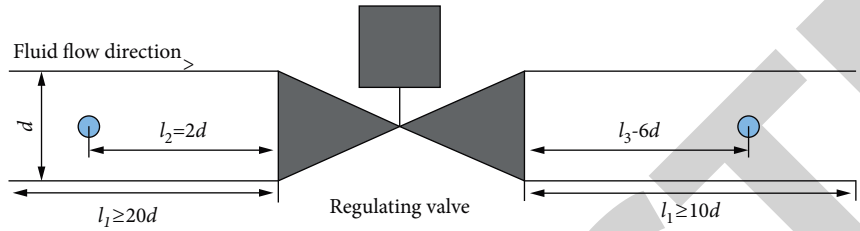

Figure 4: Nominal pipe size and adjustment position.

Table 2: Variation of opening and flow coefficient.

Openness (%0)	Δp (kPa)	μt/°	Cv	FL	
0	99.99	0.95	1.74	20.81	21.6
5	99.95	0.94	2.07	16.32	21.6
10	99.91	0.94	2.51	13.14	21.6
15	99.87	0.94	3.06	9.86	21.6
20	98.33	0.94	3.72	5.97	21.6
25	97.59	0.93	4.52	4.34	21.6
30	92.14	0.93	5.50	3.09	21.6
35	85.86	0.93	6.68	2.65	21.6
40	77.23	0.93	8.13	1.98	21.6
45	69.15	0.92	9.89	1.43	21.6
50	59.31	0.92	12.02	1.19	21.6
55	52.42	0.92	14.62	0.87	21.6
60	44.82	0.92	17.78	0.69	21.6
65	36.37	0.91	21.62	0.61	21.6
70	31.95	0.91	26.29	0.55	21.6
75	23.08	0.91	31.97	0.48	21.6
80	18.46	0.91	38.87	0.43	21.6
85	12.79	0.90	47.27	0.36	21.6
90	8.03	0.90	57.48	0.30	21.6
95	6.62	0.90	69.90	0.23	21.6
100	3.54	0.90	85.00	0.19	21.6

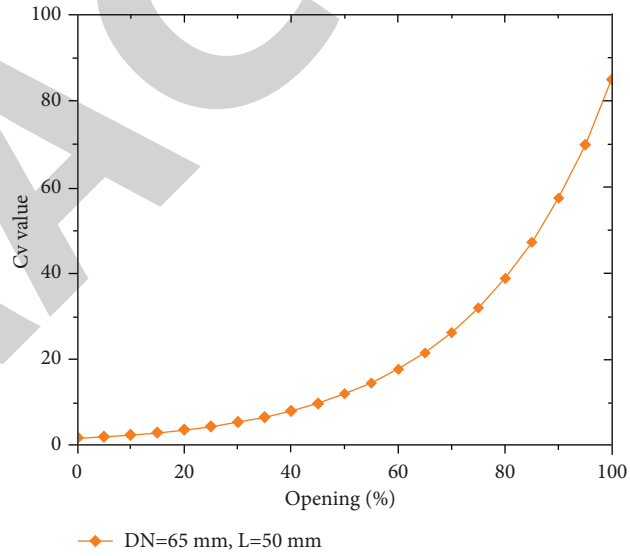

Figure 5: Control valve flow characteristic curve.

Solidworks Flow Simulation fluid dynamics simulation was performed to calculate and analyze parameters such as velocity, pressure, and vortex at 20% and 100% opening. The medium used is water vapor, having density of 0.6 kg/m^3, temperature of 20.05°C, and inlet velocity of 0.5 m/s, with static outlet pressure.

The pressure, velocity, flow traces, and vortex clouds are shown in Figures 9–12 for a 20% opening (small opening of the regulating valve).

From Figure 9, the maximum pressure of fluid in the valve cavity is 0.066 MPa, and the pressure decreases in steps through the curved cage and the noise reduction cage. It shows that the curved cage and the noise reduction cage not only reduce the noise by pressure change but also control the flow rate. The pressure around the inner side of the spool is evenly distributed, and the spool is evenly and firmly stressed. From Figures 10 and 11, the fluid from the valve cavity from bottom to top flows through the long neck area and noise reduction hole; when entering the long neck area of the long neck window, the circulation area decreases, and the maximum speed is 1.642 m/s; after flowing through the noise reduction hole, the speed drops to 0.076 m/s; after flowing through the curve valve cage and noise reduction valve cage, there is no significant change in speed compared with the flow. It shows that the flow velocity is uniform, the flow resistance is small, the control valve is stable, there is vibration damping, and the noise reduction effect is good. From Figure 12, the maximum value of vortex 278.161/s is located at the contact point between the small short neck window and the spool, and the vortex in the valve cavity and the inlet and outlet is low, indicating that the long and short neck windows and noise reduction holes reduce noise and play a role in noise reduction.

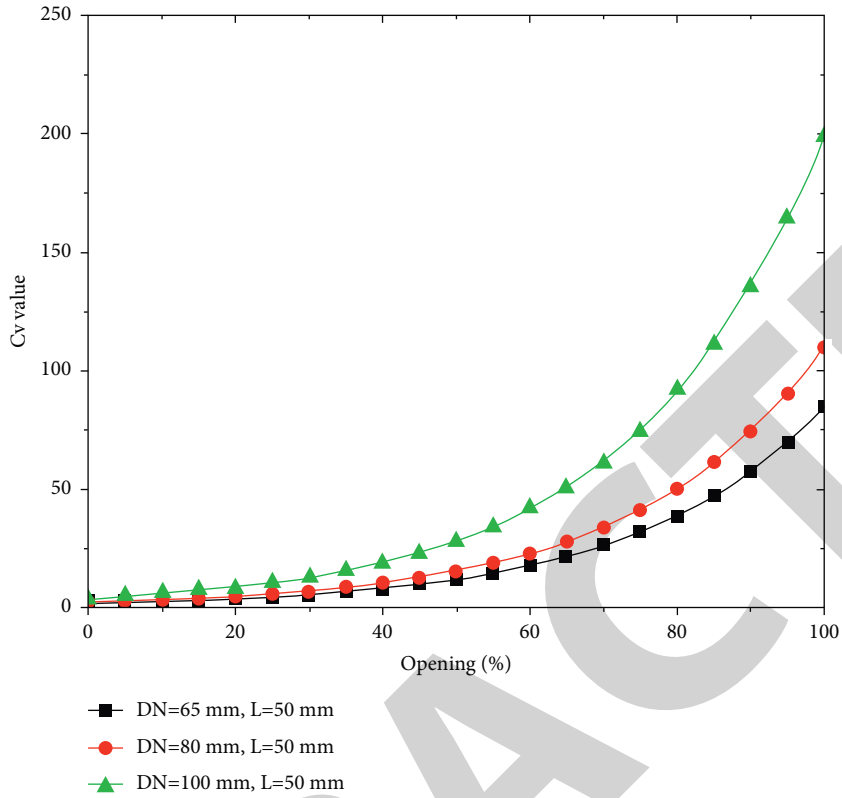

Figure 6: Variation of Cv with nominal diameter for the same stroke.

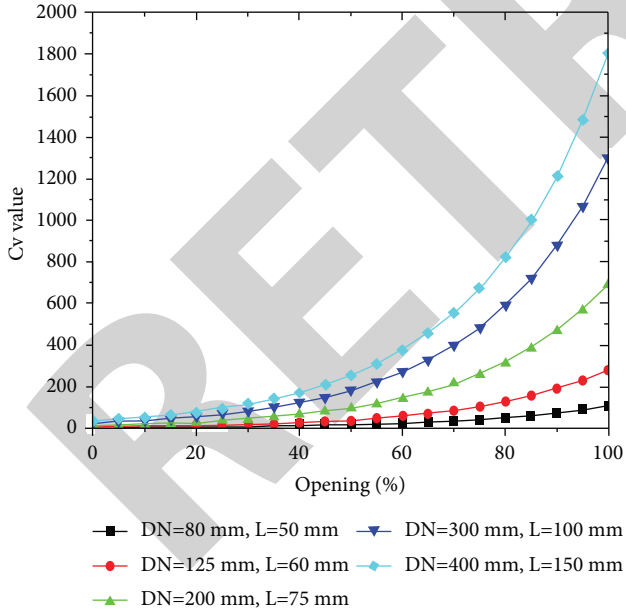

Figure 7: Variation of Cv for different strokes with different nominal diameters.

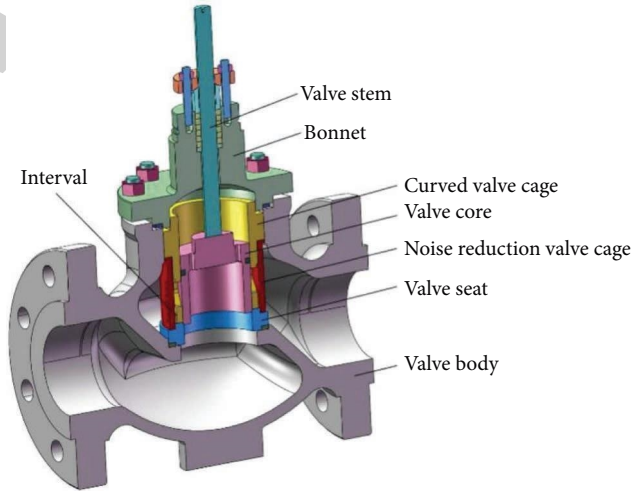

Figure 8: Ball valve model.

The pressure, velocity, flow traces, and vortex clouds are shown in Figures 13–16 for a 100% opening (fully open regulating valve).

Figure 13shows that the maximum pressure of the fluid in the valve chamber is 0.016 MPa. It can be seen that the fluid pressure of the long and short neck windows at the curve valve cage drops to 0.0004 MPa, and the fluid pressure between the right side of the noise reduction valve cage and the upper outlet of the valve chamber is also negative, which indicates that the fluid force is suction, the lower pressure is positive, and fluid flows out. The curved cage and the noise-reducing cage are shown to be effective in reducing noise through pressure changes while controlling flow. The pressure around the spool is evenly distributed and the force is evenly distributed, so there is no twisting force caused by uneven pressure. From Figures 14 and 15, the fluid from the valve cavity from bottom to top flows through the long and

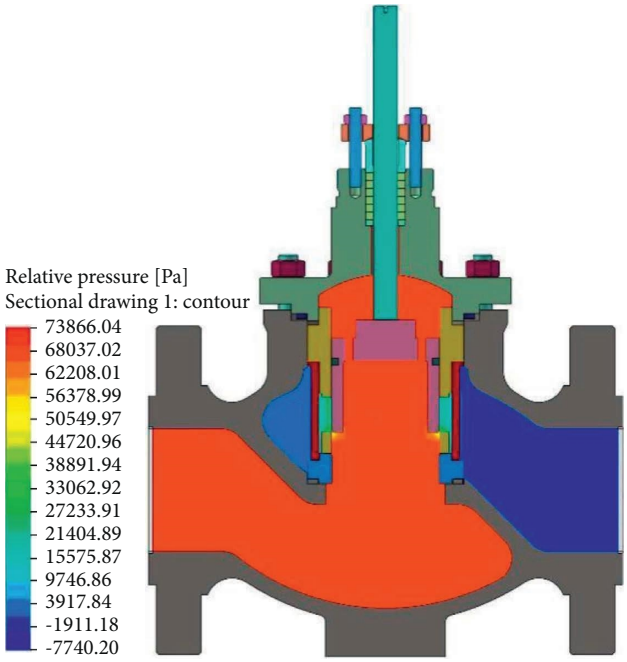

Figure 9: Pressure cloud chart for 20% opening.

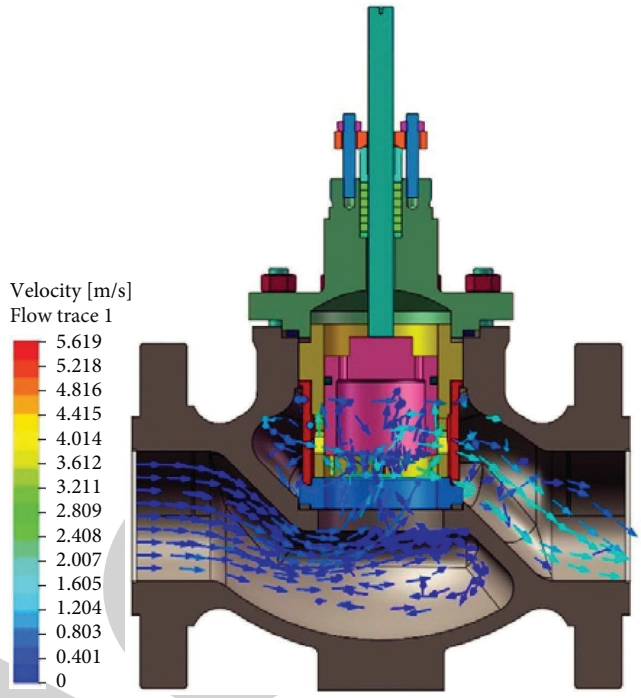

Figure 11: Flow trace diagram for 20% opening.

Figure 10: Speed cloud map for 20% opening.

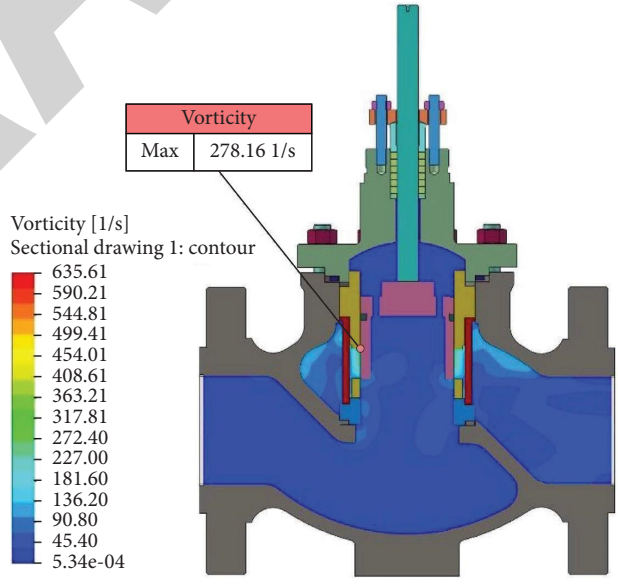

Figure 12: Vortex volume cloud map for 20% opening.

short neck area and noise reduction hole, and the maximum speed of fluid is 0.994 m/s, which is located in the middle area of the valve seat; after flowing through the noise reduction hole, the flow rate is 0.122 m/s, and the flow rate is significantly reduced. It shows that the long and short neck windows and noise reduction holes are evenly distributed, which makes the fluid beam distribution more uniform and the regulating valve smooth with effective noise reduction. From Figure 16, it can be seen that the maximum vortex flow is 125.131/s, and the vortex flow in the valve chamber, inlet, and outlet is lower than 801/s in the microgroove, which indicates that the whole valve chamber is low noise, and it can be concluded that the bending valve cage and noise reduction valve cage can significantly reduce the noise.

The inlet pressure-opening curve of the flow window on the left side of the control valve and the outlet pressure-opening curve of the noise-reducing orifice on the left side are shown in Figure 17.

Right flow window inlet pressure-opening curve and right noise reduction orifice outlet pressure-opening curve are shown in Figure 18.

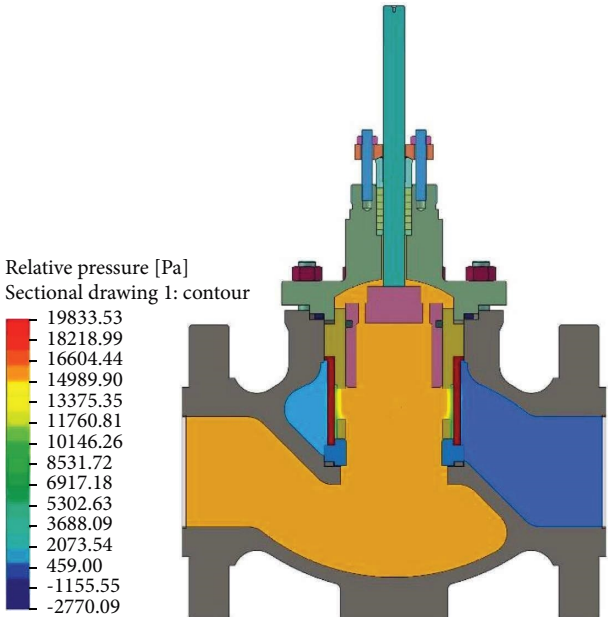

Figure 13: Pressure cloud map for 100% opening.

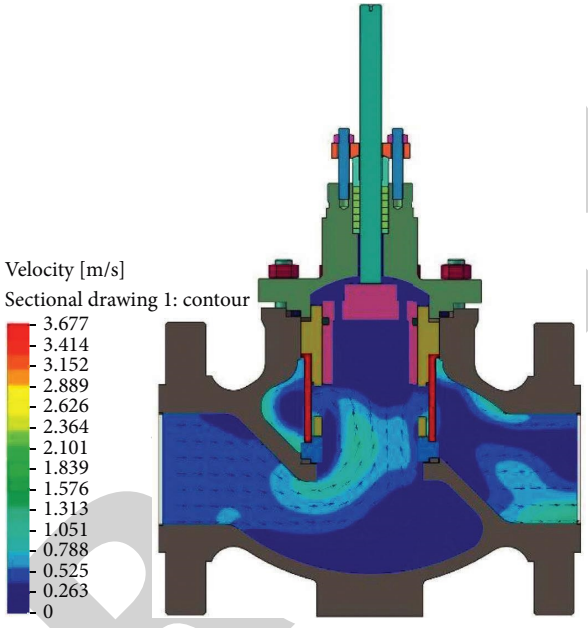

Figure 14: Speed cloud map for 100% opening.

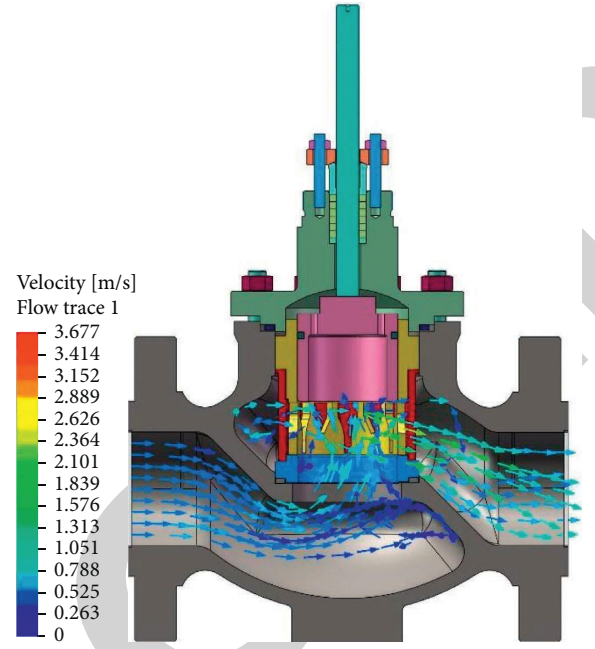

Figure 15: Flow trace diagram for 100% opening.

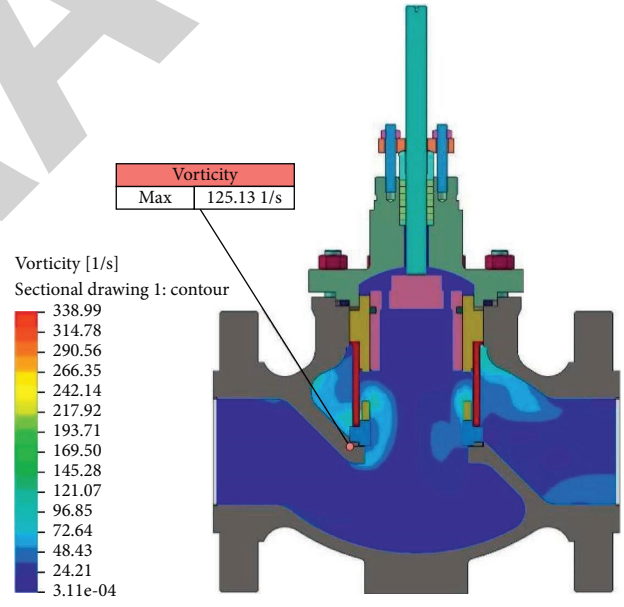

Figure 16: Vortex volume cloud map for 100% opening.

In the left and right sides of the flow window, noise reduction hole fluid inlet and outlet pressure increases first with the opening degree and then decreases; in the small opening degree of 5%~15%, pressure value reaches the maximum. The pressure before entering the flow window is less than the noise reduction orifice outlet pressure, and the right noise reduction orifice outlet pressure is less than the left noise reduction orifice outlet pressure, which is in line with the structural characteristics that the right side is the outlet and the pressure reduction is greater than the left side. The pressure before entering the flow window is less than the noise reduction orifice outlet pressure, and the right noise reduction orifice outlet pressure is less than the left noise reduction orifice outlet pressure, which is in line with the structural characteristics that the right side is the outlet and the pressure reduction is greater than the left side. It shows that the flow window and the noise reduction orifice make the pressure before and after the fluid change, and the pressure reduction makes the internal force of the fluid and the force of the fluid on the valve cavity reduce, the flow is regulated, and the noise is reduced.

The inlet velocity-opening curve of the left flow window and the outlet velocity-opening curve of the left noise reduction orifice are shown in Figure 19.

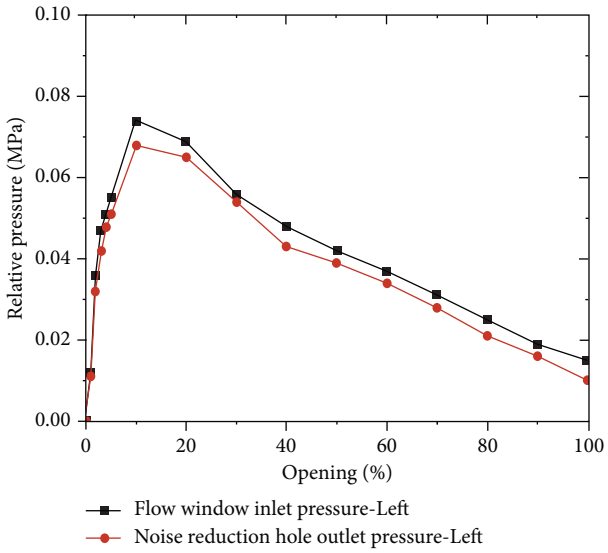

Figure 17: Pressure-opening curve at the inlet and outlet of the left flow window noise reduction orifice.

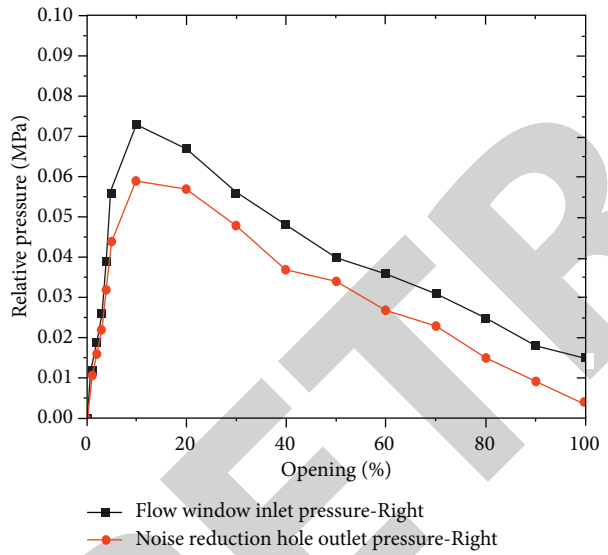

Figure 18: Right flow window noise reduction orifice inlet and outlet pressure-opening curve.

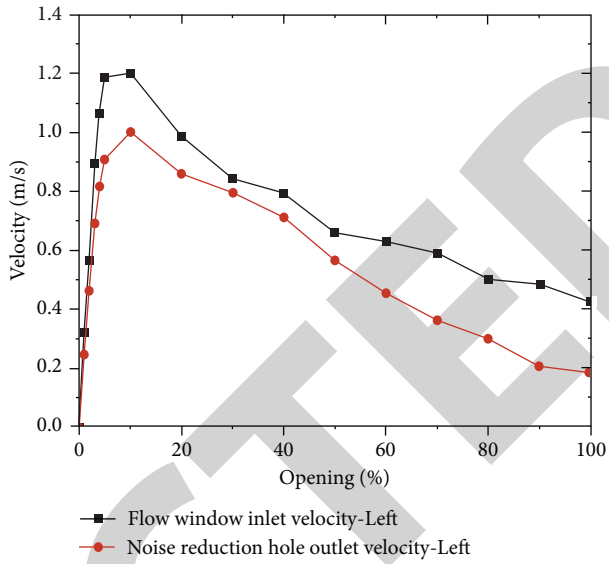

Figure 19: Left flow window noise reduction orifice inlet and outlet velocity-opening curve.

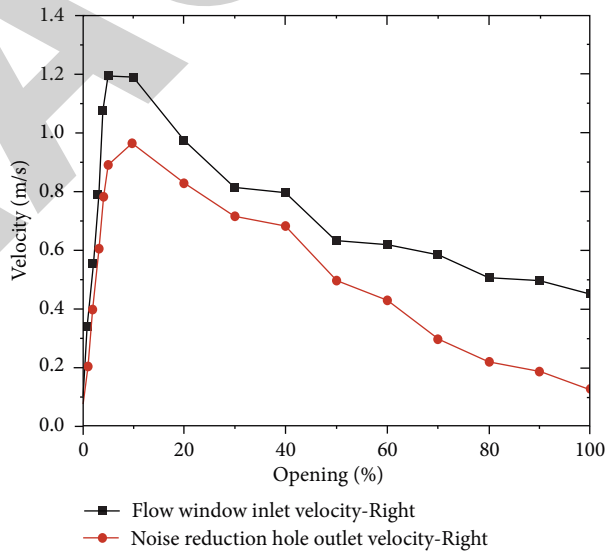

Figure 20: Right flow window noise reduction orifice inlet/outlet velocity-opening curve.

The inlet velocity-opening curve of the right flow window and the outlet velocity-opening curve of the right noise reduction orifice are shown in Figure 20.

The velocity of fluid in and out of the noise-reducing orifice on the left and right sides of the flow window also increases with the opening degree and then decreases, reaching the maximum velocity value at a small opening degree of 5% to 15%. The flow rate changes before and after the flow window and noise reduction orifice, the internal velocity of the fluid is reduced, and the reduced flow rate not only regulates the flow rate but also reduces the noise.

The vortex curve of the noise-reducing two-stage cage control valve is shown in Figure 21.

From Figure 21, the vortex volume increases and then decreases with the increase of the opening degree. The vortex volume is large at small opening of 5%~10% and decreases exponentially and rapidly at opening of 10%~25%; at opening of 25%~40%, the vortex volume continues to decrease; at opening of 40%~100%, the vortex volume changes very little and tends to be constant. At large opening, the flow rate is larger, but the vortex movement changes very little, and the regulating valve still operates stably.

The drag coefficient curve of the noise-reducing two-stage cage control valve is shown in Figure 22.

From Figure 22, the test and simulation results show the same trend, the drag coefficient decreases with the increase of opening degree. The resistance coefficient is large at small opening and decreases rapidly in exponential form at 0%–25% opening; at 25%–50% opening, the resistance coefficient

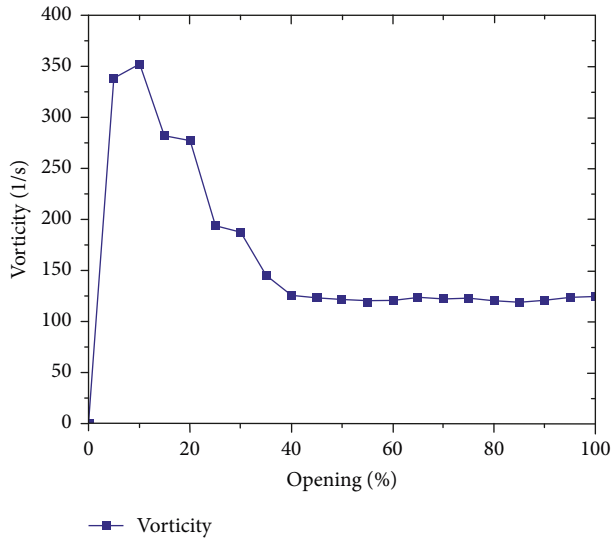

Figure 21: Vortex volume curve.

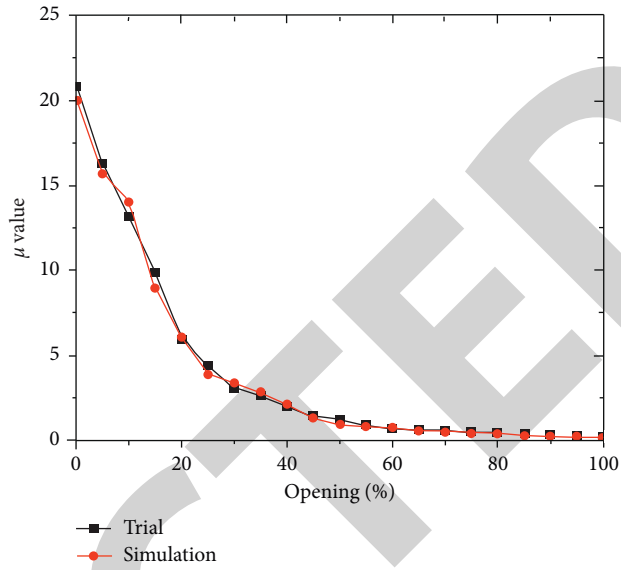

Figure 22: Resistance coefficient curve.

decreases continuously, but at a slower rate; at 50%–100% opening, the resistance coefficient changes very little and remains basically stable. The effect of curved valve cage and noise-reducing valve cage on the resistance coefficient of the regulating valve is larger at small openings, and the effect on the resistance coefficient of the regulating valve is relatively small at large openings. At small opening, the flow resistance is small, the flow rate is small, and the regulating valve operates stably.

4.4. Cavitation Properties of Air Cavities

4.4.1. Air Cavitation Analysis. Liquid flows through the regulating valve due to the throttling effect, and the flow rate and pressure at the throttle port will be a sharp change. When the pressure reaches or is lower than the fluid temperature, part of the liquid vaporizes into bubbles, and sublimation occurs. The fluid is in a gas-liquid two-phase state. When the fluid leaves the throttle valve, the pressure rises, which is greater than the saturated steam pressure, and the bubble breaks into liquid. Vapor forms cavitation, which is the main factor to generate flow noise and affects the stability and service life of the regulating valve.

The magnitude of cavitation generation is measured by the cavitation coefficient, σ_c:

$$\sigma_c = \frac{p_2 - p_v}{p_1 - p_2}, \tag{6}$$

where σ_c is the air cavity coefficient, p_2 is the pressure at the valve, and p_v is the fluid saturated vapor pressure at the throttle.

The magnitude of the cavitation effect is measured by the cavitation coefficient. Cavitation coefficient k_a [29]:

$$K_a = \frac{p_2 - p_v}{\sigma_c (p_1 - p_v)}, \tag{7}$$

where k_a is the cavitation factor.

In the flow of noise, there are liquid power noise and gas power noise, and noise affects the performance of the regulating valve, so noise estimation is important for noise reduction. When the liquid flows, $\Delta p \le p_r$, liquid flow sound pressure level:

$$\mathrm{SPL}_0 = 10\lg\left(1.17C_{v_0}\right) + 20\lg(0.01\Delta p) - 30\lg b + 70, \tag{8}$$

where SPL_0 is the fluid dynamic noise sound pressure level, C_{v_0} is the flow coefficient at a specific flow rate, b is the pipe wall thickness, and Δp_r is the regulating valve differential pressure at the start of cavitation.

When the liquid flows, $\Delta p_r < \Delta p < \Delta p_s$, the initial cavitation sound pressure level:

$$\mathrm{SPL}_1 = 10\lg\left(1.17C_{v_0}\right) + 20\lg(0.01\Delta p) + \frac{5[\Delta p - K_a(p_1 - p_v)]}{(p_1 - p_v)\left(\mathrm{FL}^2 - K_a\right)} \cdot \lg[0.145(p_2 - p_v)] - 30\lg\varepsilon + 70, \tag{9}$$

where SPL_1 is the initial cavitation fluid flow sound pressure level, K_a is the initial cavitation factor, and Δp_s is the regulating valve differential pressure at full cavitation.

When the liquid flows, $\Delta p > \Delta p_s$, $p_2 > p_v$, fully cavitated sound pressure level:

$$\mathrm{SPL}_2 = 10\lg\left(1.17C_{v_0}\right) + 20\lg(0.01\Delta p) + \frac{5[\Delta p - K_a(p_1 - p_v]}{\left(p_1 - p_v\left(\mathrm{FL}^2 - K_a\right)\right.} \cdot \lg[0.145(p_2 - p_v)] - 30\lg\varepsilon - 5\lg[0.01(\Delta p - \Delta p_r)] + 64, \tag{10}$$

where SPL_2 is the sound pressure level of fully cavitated fluid flow.

Water vapor sound pressure level when the gas is flowing:

$$\mathrm{SPL}_3 = 10\lg\left[6.8\times10^3 C_{v_0}\mathrm{FL}p_1p_2D^2\beta\frac{(1+0.00126T_1)^6}{\varepsilon}\right], \tag{11}$$

where SPL_3 is the water vapor flow sound pressure level, D is the diameter of pipe downstream of control valve, β is the audio efficiency, and T_1 is the steam superheat temperature.

Sound pressure level of gas other than water vapor when the gas is flowing:

$$\mathrm{SPL}_4 = 10\lg\left(30C_{v_0}\mathrm{FL}p_1p_2D^2\beta\frac{T_2}{\varepsilon^3}\right) + \mathrm{SL}_g, \tag{12}$$

where SPL_4 is the sound pressure level of gas flow other than water vapor, T_2 is the fluid temperature, and SL_g is the gas characteristic coefficient.

Translated withhttps://www.DeepL.com/Translator (free version):

$$M_{a1} = \frac{138W\left(1+0.00126T_1\right)}{p_2d^2}, \tag{13}$$

where M_{a1} is the Mach number of water steam outlet of control valve, W is the water vapor mass flow rate, and d is the control valve outlet diameter.

Control valve outlet diameter:

$$\mathrm{SPL}_5 = 10\lg\left[\frac{0.0208p_2^2d^2D^2M^8a_1\left(1+0.001267T_1^6\right)}{\varepsilon^3}\right], \tag{14}$$

where SP_5 is the control valve outlet water vapor sound pressure level.

Mach number of gases other than water vapor:

$$M_{a2} = \frac{6.2U_1\sqrt{\varepsilon T_2}}{p_2d^2}, \tag{15}$$

where M_{a2} is the Mach number of gas other than water vapor at the outlet of the control valve U_1 is the water vapor volume flow rate.

Sound pressure level of gases other than water vapor:

$$\mathrm{SPL}_6 = 10\lg\left(\frac{2.8p_2^2d^2D^2M^8a_2T_2}{10^4\varepsilon^3}\right) + SL_g, \tag{16}$$

where SPL_6 is the sound pressure level of gas other than water vapor at the outlet of control valve.

4.4.2. Cavitation Simulation Analysis. The cavitation phenomenon will generate vibration and noise, which affects the noise reduction of the regulating valve, so it is especially important to study the cavitation phenomenon. The model of the regulating valve is imported into Solidworks Simulation 2021, and the simulation model is shown in Figure 23.

Water at 90°C flows through the pipe at a speed of 4 m/s. The water flow is partially blocked in the middle by the spool, curved cage, and noise reduction cage, and the flow velocity and pressure drop are changed. The fluid density, Mach number, and acoustic pressure energy level clouds are shown in Figures 24–26 for 20% opening of the control valve.

The regulating valve opening (40%) fluid density cloud, Mach number cloud, and acoustic pressure energy level cloud are shown in Figures 27–29.

The 60% fluid density cloud, Mach number cloud, and acoustic pressure energy level cloud of the regulating valve opening are shown in Figures 30–32.

The regulating valve opening (80%) fluid density cloud, Mach number cloud, and acoustic pressure energy level cloud are shown in Figures 33–35.

With opening of 20%, 40%, 60%, and 80%, it is clear from Figures 24, 27, 30, and 33 that the fluid density in the pipe and ball valve is uniformly distributed and there are no areas of reduced density; therefore, no cavitation is generated in the pipe and ball valve by fluid flow. From Figures 25, 28, 31, and 34, we know that the maximum values of Mach number are 0.00632, 0.00561, 0.00546, and 0.00551, respectively, which are less than 1 and very small, indicating that the flow velocity is very low and the noise is very small. From Figures 26, 29, 30, and 35, the maximum values of acoustic energy level are 35.87 dB, 16.92 dB, 17.05 dB, and 16.73 dB, respectively, the acoustic energy level of 20% opening is below 40 dB, the acoustic energy levels of 40%, 60%, and 80% opening are below 20 dB, and the acoustic energy level of each opening is low, indicating that the noise is very small. The regulating valve is a quiet environment when working.

Opening of 20%, temperature variation, and inlet velocity vs. average fluid density curve are shown in Figure 36.

Opening of 20%, inlet velocity variation, and temperature vs. average fluid density curve are shown in Figure 37.

For the opening degree of 20%, in the case of constant opening degree, the temperature remains the same, and the average density increases with the inlet speed; at this time, the inlet speed should be increased to increase the average density of fluid to avoid cavitation. Noise reduction double-stage cage control valve small opening average density change is small, and cavitation is difficult to produce.

Opening of 100%, temperature variation, and inlet velocity vs. average fluid density curve are shown in Figure 38.

Opening of 100%, inlet velocity variation, and temperature vs. average fluid density curve are shown in Figure 39.

The opening degree is 100%; in the case of constant opening degree, the temperature remains unchanged, and the average density decreases with the increase of inlet speed; at this time, the inlet speed should be properly reduced to avoid the rapid decrease of the average density of the fluid, resulting in cavitation; the inlet speed remains unchanged, and the average density remains constant with the increase of temperature. Although the average density decreases with the increase of inlet velocity when the noise reduction double-stage cage control valve is opened at large degrees, the average density changes are small, and it is difficult to generate air pockets.

Constant inlet velocity, varying temperature, and opening vs. average fluid density curve are shown in Figure 40.

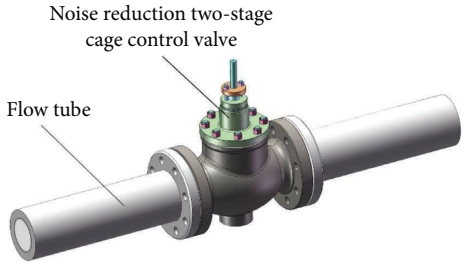

Figure 23: Calculation model of cavitation simulation.

Temperature vs. average fluid density curve with constant inlet velocity and varying opening is shown in Figure 41.

The inlet speed is constant, the temperature is constant, the average density increases with the opening degree, the opening degree increases, the flow capacity increases, and the flow rate increases; the opening degree is constant, and the average density changes very little with the increase in temperature and basically tends to remain the same. Noise reduction double-stage cage control valve inlet speed is constant, the average density change is small, and cavitation is difficult to produce.

With constant temperature and varying opening, the inlet velocity vs. average fluid density curve is shown in Figure 42.

With constant temperature and varying inlet velocity, the opening vs. average fluid density curve is shown in Figure 43.

The temperature remains unchanged, the opening degree is 20%, the inlet speed is 3.5 m/s~4.0 m/s, and the average density decreases with the increase of inlet speed; at this time, the inlet speed should be increased so that the inlet speed is greater than 4 m/s to improve the average density and avoid cavitation, the inlet speed is 4.0 m/s~6.0 m/s, and the average density increases with the increase of inlet speed; the opening degree is 40%, 60%, and 80%. The average density decreases as the inlet speed increases; at this time, the inlet speed should be reduced to avoid cavitation generation. The average density increases with the increase of opening degree and the increase gradually decreases, the average density remains unchanged with the increase of opening degree, the average density decreases with the increase of opening degree, the average density decreases with the increase of opening degree and the decrease gradually increases, and the opening degree should be reduced at this time to avoid cavitation; for the opening degree of 40%~80%, the average density increases with the increase of opening degree. Noise-reducing two-stage cage control valve temperature remains unchanged, the average density change is small, and cavitation is difficult to produce.

The size of the cavitation coefficient determines the size of the possibility of cavitation generation; the smaller the cavitation effect, the smaller the noise generated. With constant nominal diameter and varying inlet velocity, the cavitation coefficient varies with the opening curve, as shown in Figure 44.

For the inlet velocity of 3.5 m/s, 4.0 m/s, and 4.5 m/s, the cavitation coefficients are lower than 0.5, indicating that the inlet velocity is lower than 5 m/s; regardless of the opening degree, cavitation is not generated. At the inlet velocity of 5.0 m/s, the cavitation coefficient is greater than 0.5 for 20% and 40% opening and less than 0.5 for 60% and 80% opening, indicating that cavitation will be generated under small opening, which should increase the opening and reduce the cavitation coefficient, and cavitation will not be generated under large opening. The cavitation coefficient is higher than 0.5 when the inlet speed is 5.5 m/s and 6.0 m/s. The smaller the opening degree, the larger the cavitation coefficient, indicating higher possibility of cavitation, and the larger the opening degree, the smaller the cavitation coefficient, indicating smaller possibility of cavitation.

The variation curve of cavitation coefficient with inlet velocity for nominal diameter change and regulating valve half open is shown in Figure 45.

The cavitation coefficients of DN80, DN125, DN200, DN300, and DN400 nominal diameter control valves are lower than 0.5 when the inlet velocity is 3.5 m/s~5 m/s, indicating that the inlet velocity is lower than 0.5 m/s and no cavitation will occur for each nominal diameter control valve. The cavitation coefficients of DN80, DN125, and DN200 nominal diameter control valves increase with the inlet speed from 5 m/s to 6 m/s. The cavitation coefficients of DN300 and DN400 control valves also increase with the inlet speed, but the increase is smaller and the cavitation coefficients are less than 0.5, indicating that the smaller the nominal diameter is, the easier the cavitation occurs. The smaller the nominal diameter is, the easier the cavitation is generated; if the cavitation coefficient is greater than 0.5, it should increase the nominal diameter, reduce the cavitation coefficient, and reduce the possibility of cavitation.

The variation curve of cavitation coefficient with inlet velocity for nominal diameter change and full opening of regulating valve is shown in Figure 46.

The cavitation coefficients of DN80, DN125, DN200, DN300, and DN400 nominal diameter control valves are lower than 0.5 when the noise-reducing two-stage cage control valve is fully open and the inlet speed is 3.5 m/s~5 m/s, indicating that no cavitation occurs for each nominal diameter control valve. For the inlet speed of 5 m/s~6 m/s, the cavitation coefficient of nominal diameter DN80, DN125, DN200, DN300, and DN400 control valves increases with the increase of inlet speed; the smaller the nominal diameter, the greater the increase.

5. Test

In order to verify the effective noise reduction, flow control, equal percentage flow characteristic adjustment, and other functions of the noise reduction two-stage cage control valve, this chapter tests the control valve operation, valve small opening vibration, oscillation, valve element stress, and other factors.

5.1. Test Conditions. The test object is the control valve. Its specific parameters are diameter DN350, rated stroke 150 mm, rated flow coefficient 1600, nominal pressure PN20, pressure class 150, and leakage class IV. It is pneumatically

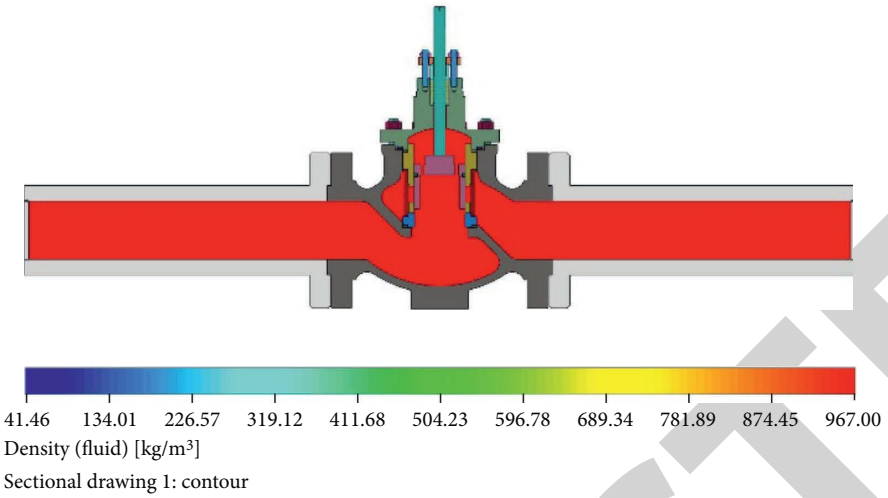

Figure 24: Fluid density cloud for 20% opening.

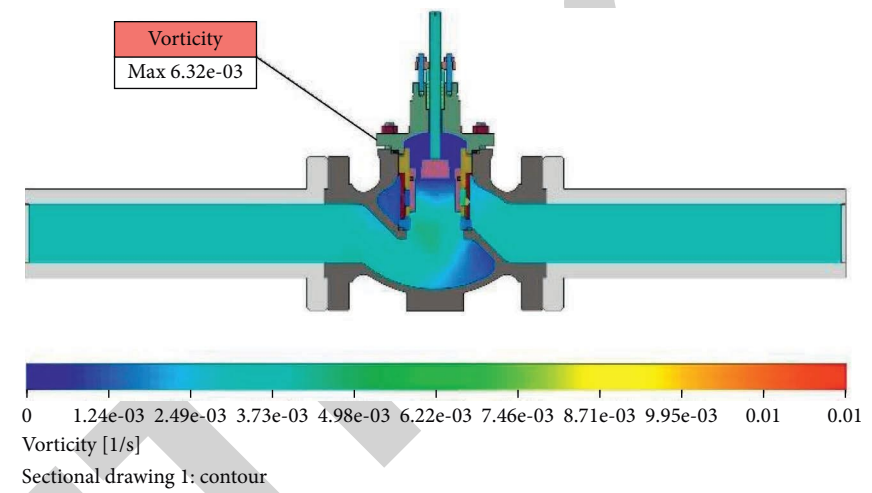

Figure 25: Mach number cloud map for 20% opening.

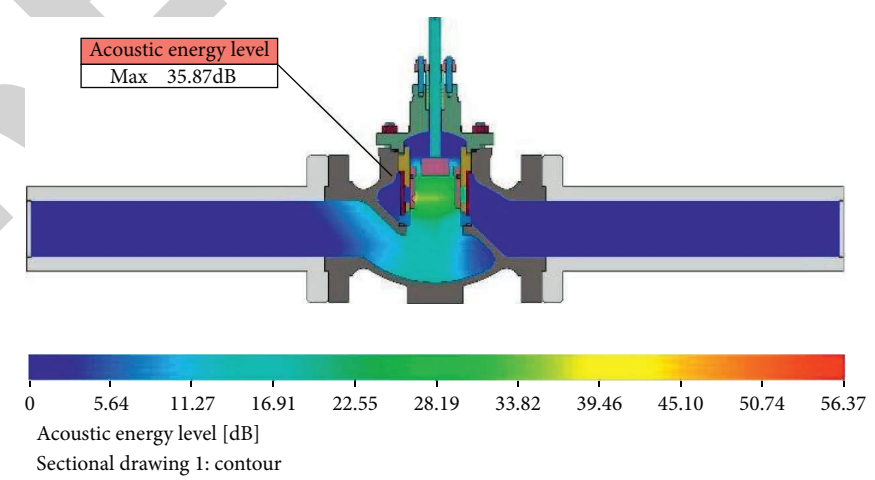

Figure 26: Acoustic energy level cloud map for 20% opening.

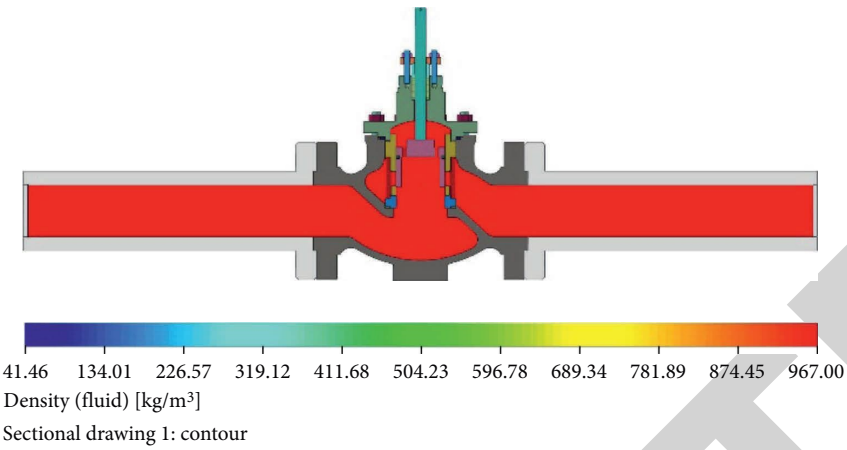

Figure 27: Fluid density cloud map for 40% opening.

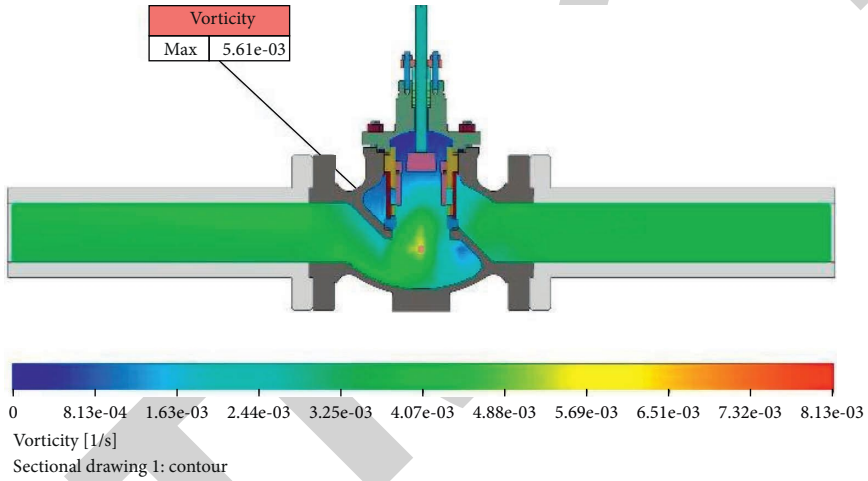

Figure 28: Mach number cloud map for 40% opening.

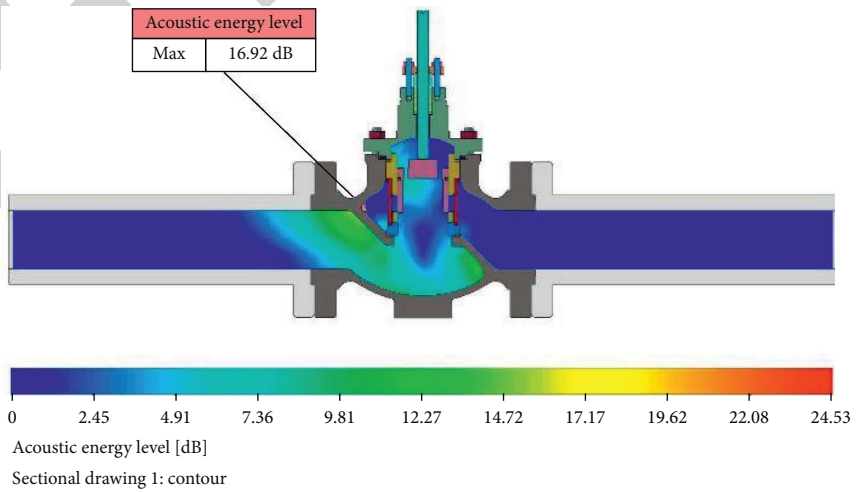

Figure 29: Acoustic energy level cloud map for 40% opening.

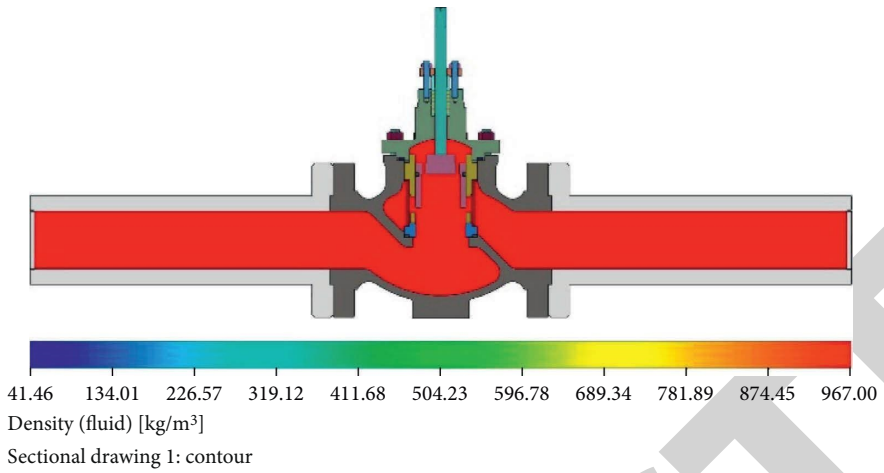

Figure 30: Fluid density cloud map for 60% opening.

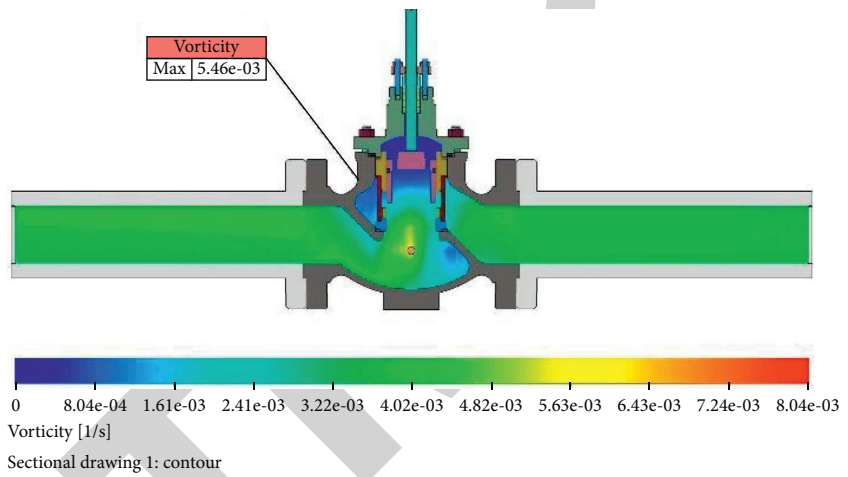

Figure 31: Mach number cloud map for 60% opening.

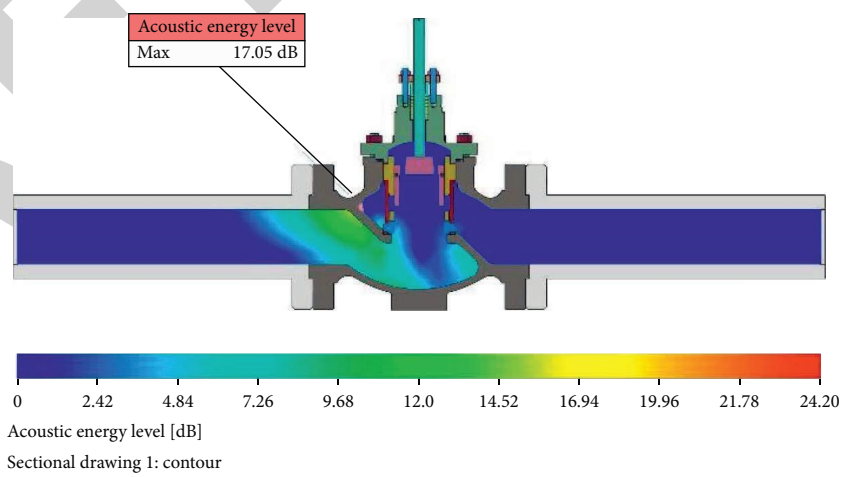

Figure 32: Acoustic energy level cloud map for 60% opening.

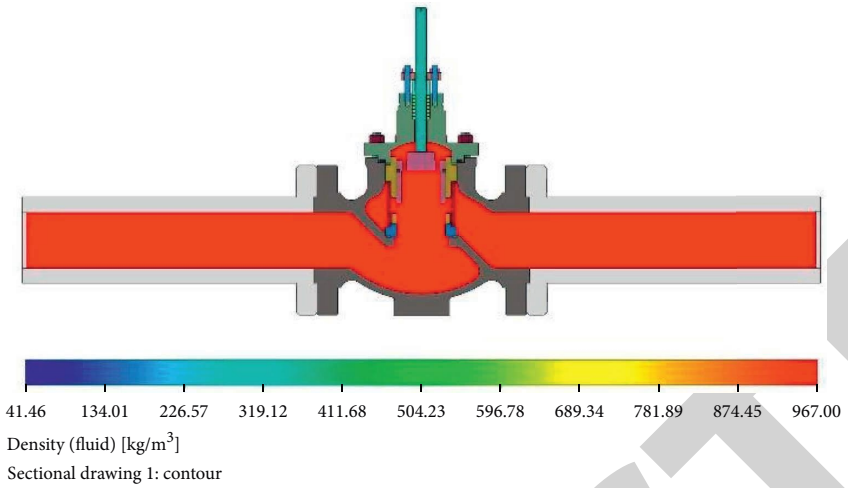

Figure 33: Fluid density cloud map for 80% opening.

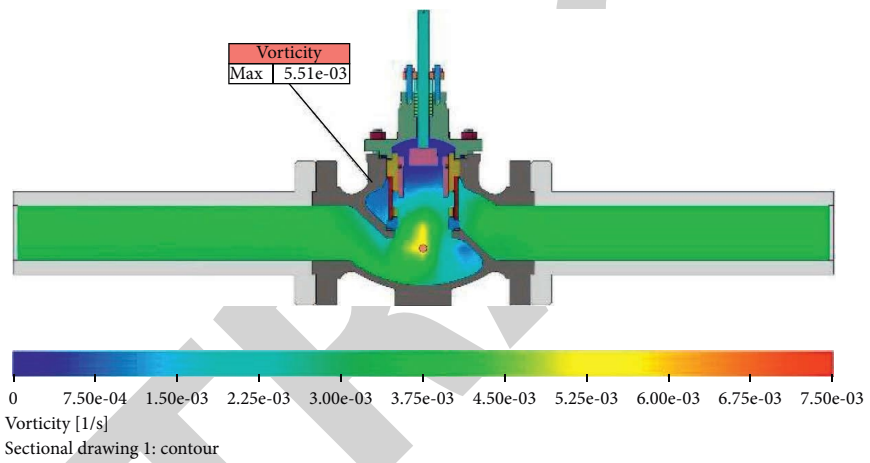

Figure 34: Mach number cloud map for 80% opening.

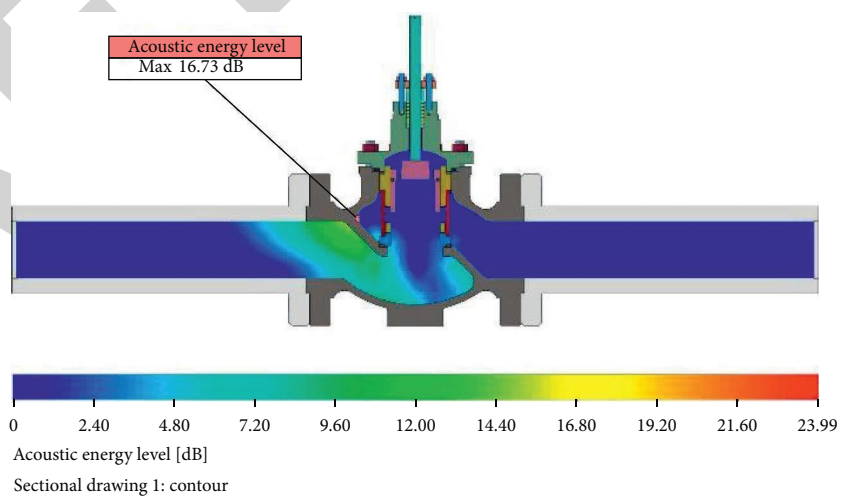

Figure 35: Acoustic energy level cloud map for 80% opening.

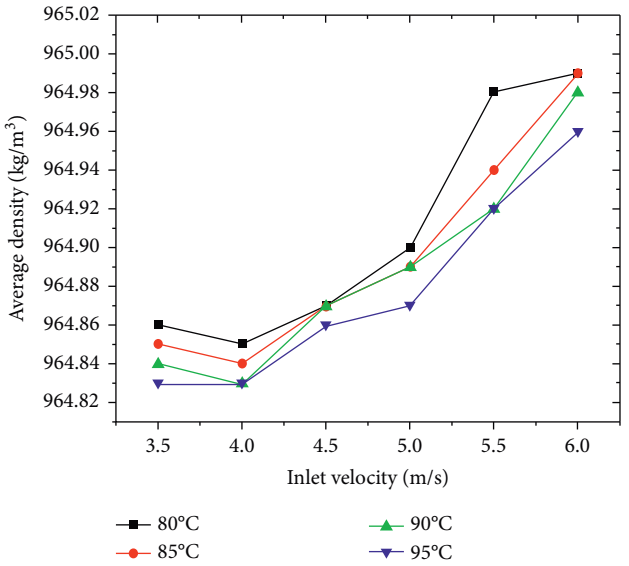

Figure 36: Inlet velocity and average density with temperature for 20% opening.

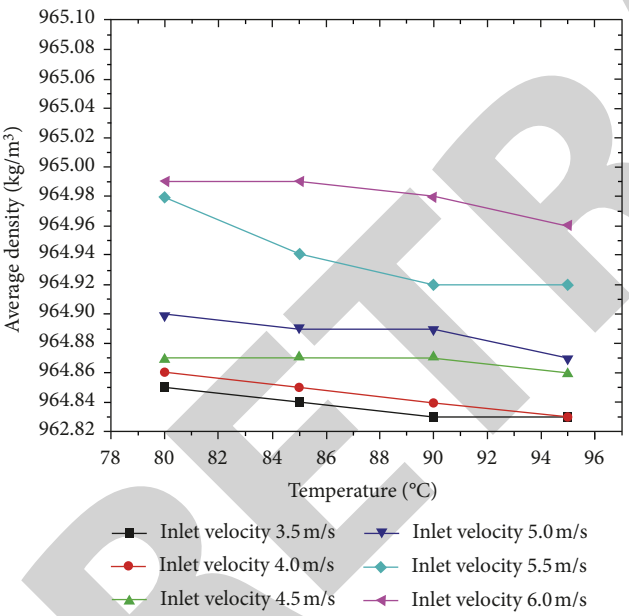

Figure 37: Temperature and average density with inlet velocity for 20% opening.

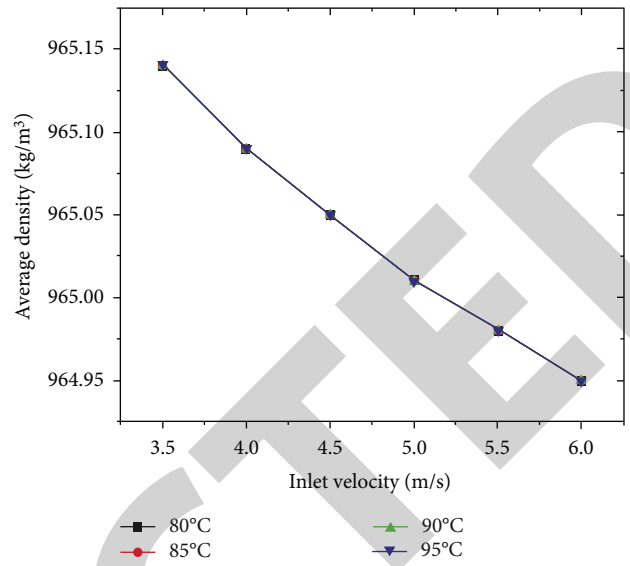

Figure 38: Inlet velocity and average density with temperature for 100% opening.

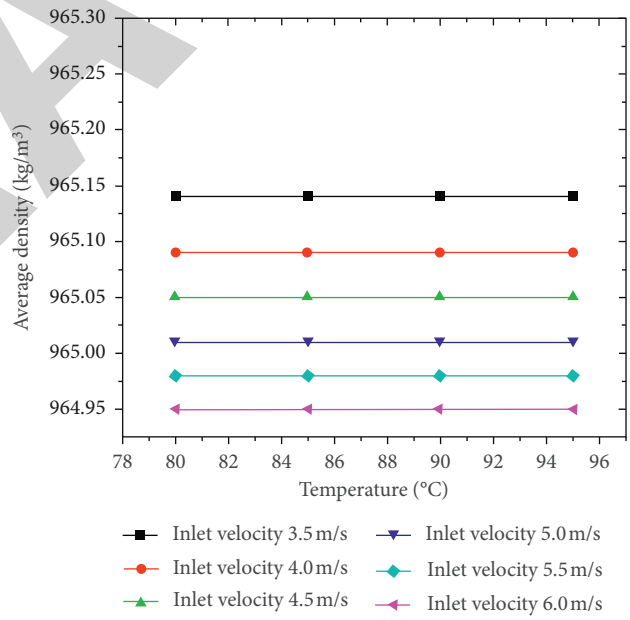

Figure 39: Inlet velocity and average density with temperature for 100% opening.

and manually driven. Test implementation standards are GB/T 4213, GB/T 13927, and ANSI FCI 70-2-2006.

The noise reduction two-stage cage control valve manufacturing prototype is shown in Figure 47.

5.2. Test Process. The control valve is installed on the test bench, the two ends of the inlet and outlet and pipeline connection fixed, the upper part is suspended by a hook fixed, the medium from the left end of the valve port flow in, the right end of the valve port out, change the medium pressurization pressure, and test the valve body pressure strength and valve cover sealing. The test is shown in Figure 48.

When testing the pressure resistance and sealing of the regulating valve, since the regulating valve can be used for both regulating and switching, a low-pressure sealing test and a high-pressure sealing test are performed on the regulating valve. The control valve noise and cavitation tests are shown in Figure 49. The control valve is installed in a piping system consisting of a throttle valve, sensor, control valve and piping, etc. The sound power level,

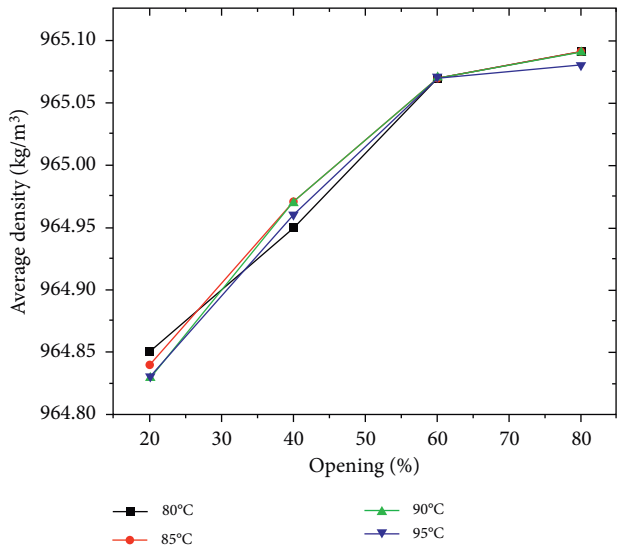

Figure 40: Variation of inlet velocity constant opening and average density with temperature.

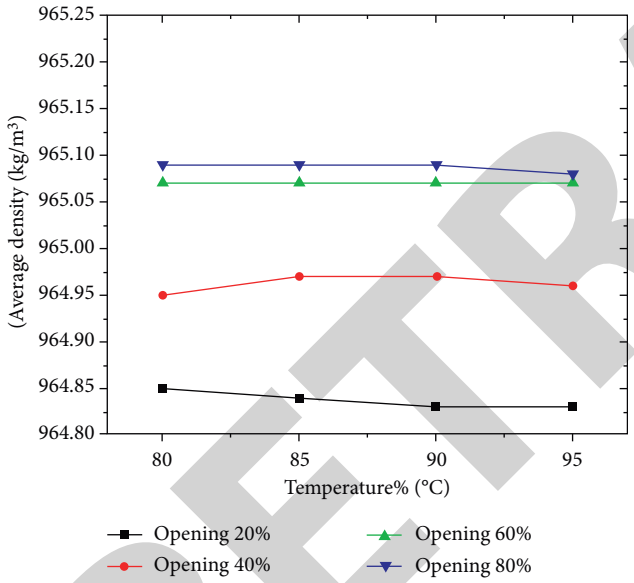

Figure 41: Variation of inlet velocity constant temperature and average density with openness.

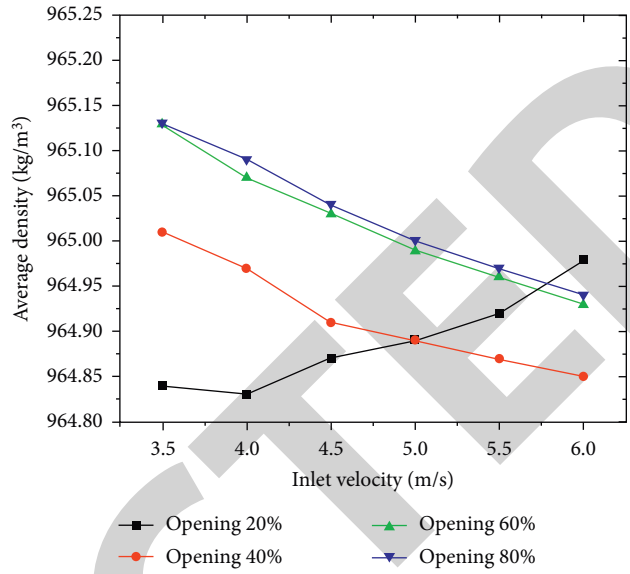

Figure 42: Variation of inlet velocity and average density with openness at constant temperature.

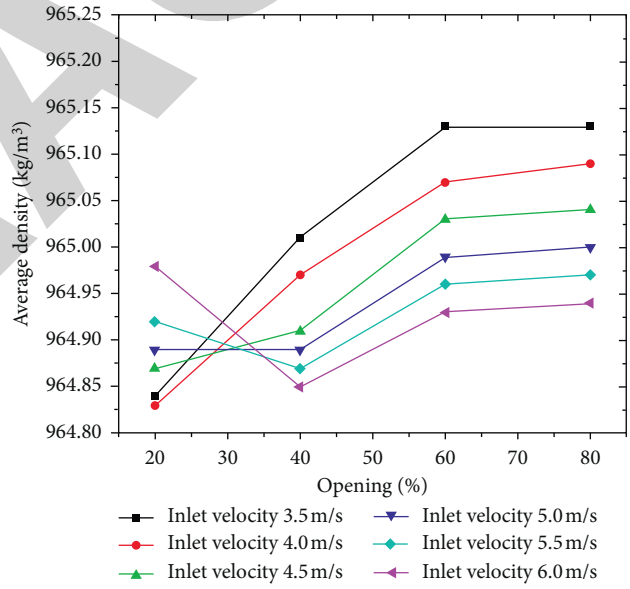

Figure 43: Variation of temperature-constant openness and average density with inlet velocity.

average density of liquid flow, and cavitation coefficient are tested.

5.3. Analysis of Test Results. The results of pressure test, low-pressure sealing test, and high-pressure sealing test of control valve are shown in Table 3.

Control valve noise and cavitation test results are shown in Table 4.

The maximum sound power level is 36.24 dB, 16.51 dB, 16.03 dB, 15.78 dB, 14.32 dB, 14.32 dB, and 13.91 dB, respectively, which are small and decrease with the increase of opening degree, indicating that the fluid flow noise is very small. It is a normal flow quiet environment. The average density of liquid flow is 966.11 kg/m^3, 965.51 kg/m^3, 965.52 kg/m^3, 965.48 kg/m^3, 965.63 kg/m^3, and 965.67 kg/m^3, respectively, and the average density changes very little with the increase of opening degree, so it is difficult to produce air pockets. The cavitation coefficients are 0.39, 0.36, 0.34, 0.31, 0.28, and 0.26, respectively, which are less than 0.5 and decrease gradually with the increase of the opening degree; therefore, no cavitation occurs.

The yield strength of each material is shown in Table 5.

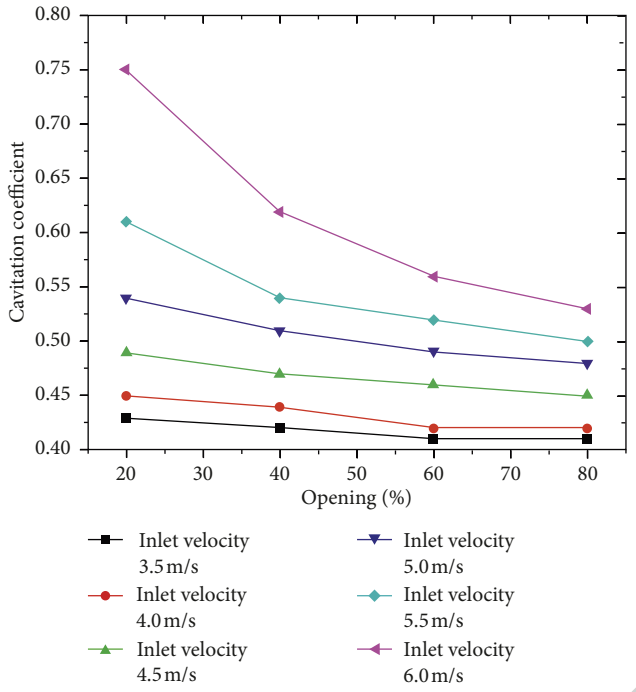

Figure 44: Nominal diameter constant opening and cavitation coefficient with inlet velocity.

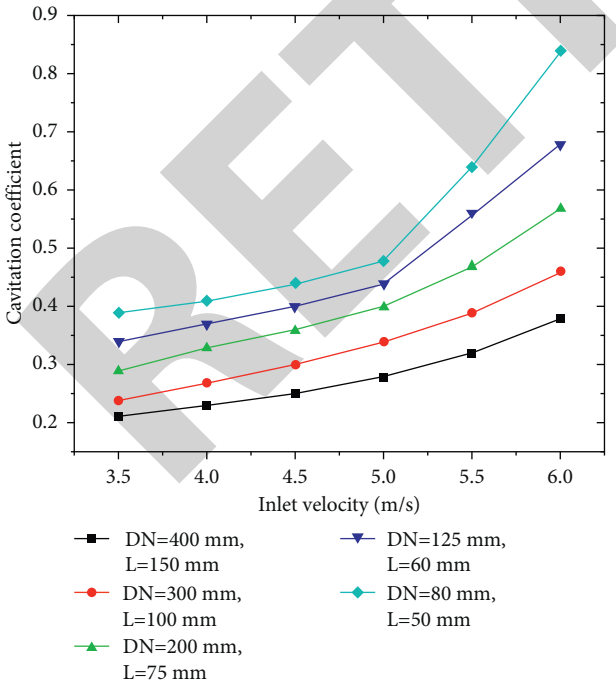

Figure 45: Variation of inlet velocity and cavitation coefficient with nominal diameter at half opening.

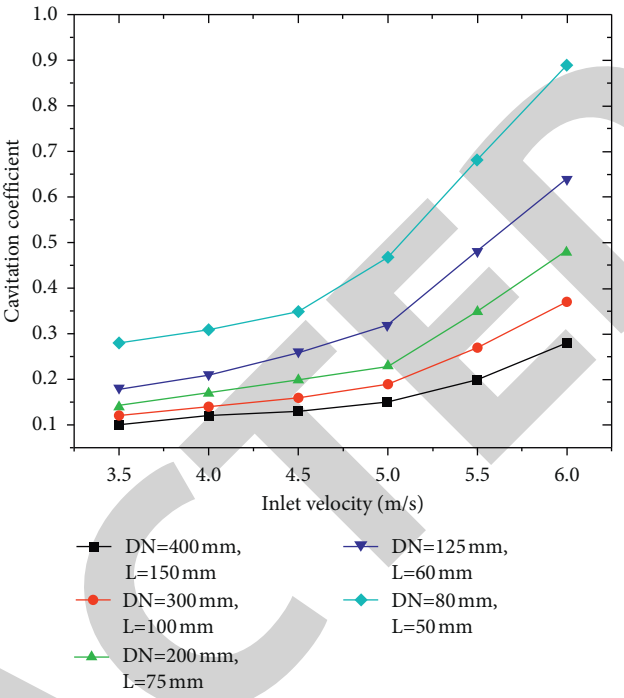

Figure 46: Variation of inlet velocity and cavitation coefficient with nominal diameter at full opening.

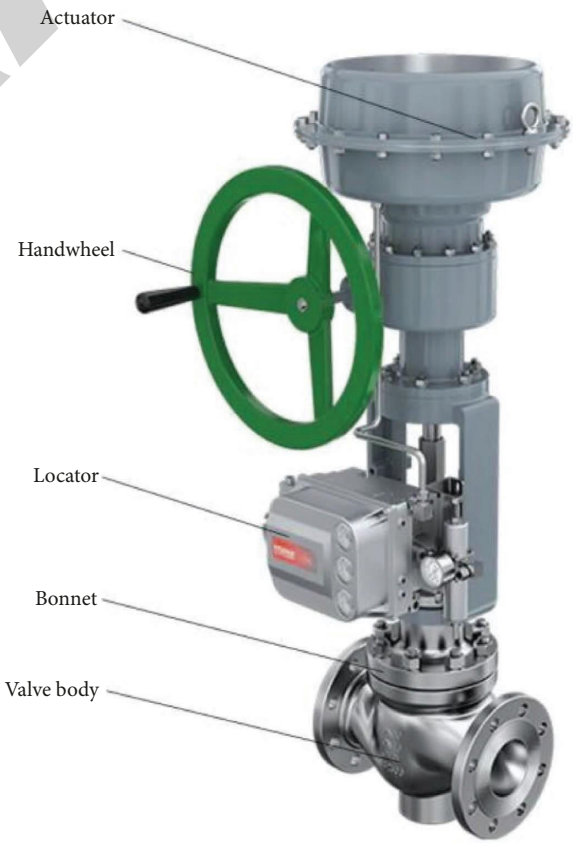

Figure 47: Noise-reducing double-stage cage control valve.

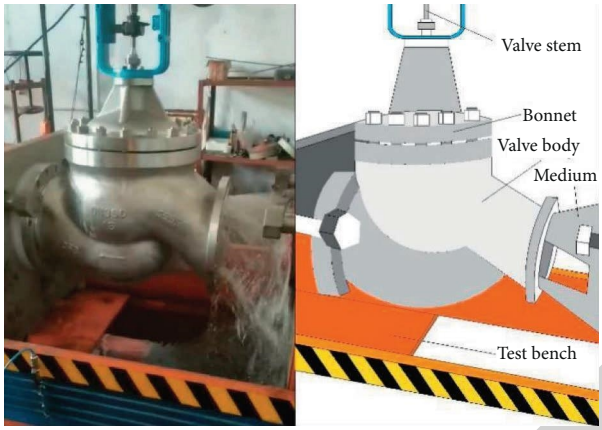

Figure 48: Noise-reducing two-stage cage control valve pressure resistance and sealing test.

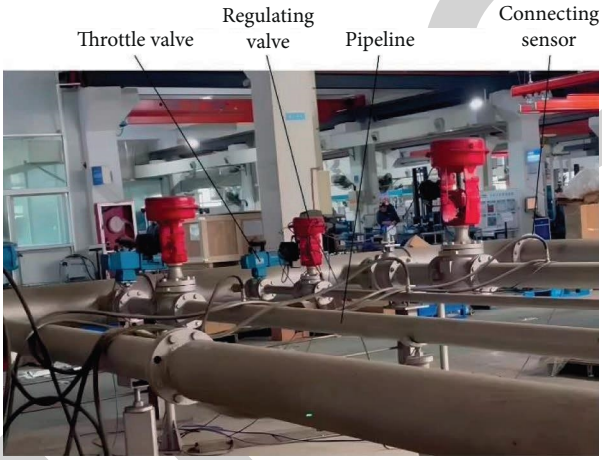

Figure 49: Control valve noise and cavitation test.

Table 3: Test results.

Test items	Valve body pressure resistance test	High-pressure sealing test	Low-pressure sealing test
Pressure setting value (MPa)	0.35	3.00	2.20
Holding time (s)	180	300	180
Leakage setting value (ml/min)	1.50	0.00	1.50
Measured leakage volume (ml/min)	0.42	0.00	0.67
Actual value of pressure (MPa)	0.36	3.02	2.20
Holding pressure drop value (MPa)	0.01	0.02	0.00

Table 4: Test results.

Openness (%)	Maximum sound power level (dB) flow (kg/m^3)	Cavitation factor	Average density of liquid
20	966.11	36.24	0.39
40	965.51	16.51	0.36
50	965.52	16.03	0.34
60	965.48	15.78	0.31
80	965.63	14.32	0.28
100	965.67	13.91	0.26

Table 5: Yield strength of each material.

Names	CF8M	LCB	420	WC6	316
Yield strength (MPa)	200	275.8	345	170	20

6. Conclusion

Noise reduction double-stage cage type control valve adopts noise reduction valve cage and curve valve cage for noise reduction, forming a two-stage noise reduction, with uniform flow rate, good diffusion effect, and good noise reduction effect, which can meet the equal percentage flow characteristics of the control valve, effectively reduce the noise generated by gas, steam, and gas-liquid medium, and can perfectly ensure the equal percentage flow characteristics of the control valve, making the process parameter (flow, pressure, temperature, etc.) regulation quality excellent. Therefore, this innovative technology has substantial features and progress compared with the prior art. The flow characteristics of the noise-reducing two-stage cage control valve are studied, and the fluid flow coefficient, the flow characteristic curve, the change of flow coefficient with nominal diameter under the same stroke, and the change of flow coefficient under different strokes with different nominal diameters are analyzed. The cavitation phenomenon of cavitation was studied, and the fluid density cloud, Mach number cloud, and acoustic pressure energy level cloud were calculated by simulation to analyze the effect of cavitation on noise. The relationship between inlet velocity and cavitation coefficient with nominal diameter at half open and the relationship between inlet velocity and cavitation coefficient with nominal diameter at full open were studied, and the cavitation generation and its effect on noise were analyzed.

In the future, we will use complete test equipment to simulate more severe test environments to test new steel body features.

Data Availability

The experimental data used to support the findings of this study are available from the corresponding author upon request.

Conflicts of Interest

The authors declare that they have no conflicts of interest.

Authors' Contributions

Yu Ruiming was responsible for conceptualization, data curation, formal analysis, software, validation, methodology, and original draft preparation. Lu Xi was responsible for supervision and project administration. All authors reviewed and approved the final manuscript.

Acknowledgments

This study was supported by the National Natural Science Foundation of China (Grant: 51975379) and the Shanghai Natural Science Foundation of China (grant no. 19ZR1435500).

References

[1] V. Hessel, P. Angeli, A. Gavriilidis, and H. Löwe, "Gas-liquid and gas-liquid-solid microstructured reactors: contacting principles and applications," *Industrial & Engineering Chemistry Research*, vol. 44, no. 25, pp. 9750–9769, 2005.

[2] A. Varvani Farahani and S. Abolfathi, "Sliding mode observer design for decentralized multi-phase flow estimation," *Heliyon*, vol. 8, no. 2, Article ID e08768, 2022.

[3] A. Tanimu, S. Jaenicke, and K. Alhooshani, "Heterogeneous catalysis in continuous flow microreactors: a review of methods and applications," *Chemical Engineering Journal*, vol. 327, no. 11, pp. 792–821, 2017.

[4] S. Keskin, D. Kayrak-Talay, U. Akman, and Ö Hortaçsu, "A review of ionic liquids towards supercritical fluid applications," *The Journal of Supercritical Fluids*, vol. 43, no. 1, pp. 150–180, 2007.

[5] Ž Knez, E. Markočič, M. Leitgeb, M. Primožič, M. Knez Hrnčič, and M. Škerget, "Industrial applications of supercritical fluids: a review," *Energy*, vol. 77, no. 11, pp. 235–243, 2014.

[6] X. Xie, X. Pan, F. Shao, W. Zhang, and J. An, "MCI-Net: multi-scale context integrated network for liver CT image segmentation," *Computers & Electrical Engineering*, vol. 101, Article ID 108085, 2022.

[7] J. Tan, Y. N. Ji, W. S. Deng, and Y. F. Su, "Process intensification in gas/liquid/solid reaction in trickle bed reactors: a review," *Petroleum Science*, vol. 18, no. 4, pp. 1203–1218, 2021.

[8] M. Ballesteros Martínez, E. Pereyra, and N. Ratkovich, "CFD study and experimental validation of low liquid-loading flow assurance in oil and gas transport: studying the effect of fluid properties and operating conditions on flow variables," *Heliyon*, vol. 6, no. 12, Article ID e05705, 2020.

[9] X. Nie, Y. Zhu, and L. Li, "The flow noise characteristics of a control valve," *The Open Mechanical Engineering Journal*, vol. 8, no. 1, pp. 960–966, 2014.

[10] J. Zhang, Q. Yang, R. Lv, B. Liu, and Y. Li, "Research on noise generation mechanism and noise reduction ball valve measures of ball valve," *IEEE Access*, vol. 8, no. 1, Article ID 15973, 2020.

[11] A. S. Prakash, K. S. Ram, and V. R. Kishore, "Aeroacoustics analysis of globe control valves," *International Journal of Automotive and Mechanical Engineering*, vol. 15, no. 3, pp. 5547–5561, 2018.

[12] L. F. Zeng, G. W. Liu, J. R. Mao et al., "Flow-induced vibration and noise in control valve," *Proceedings of the Institution of Mechanical Engineers-Part C: Journal of Mechanical Engineering Science*, vol. 229, no. 18, pp. 3368–3377, 2015.

[13] W. Xu, Q. Wang, D. Wu, and Q. Li, "Simulation and design improvement of a low noise control valve in autonomous underwater vehicles," *Applied Acoustics*, vol. 146, no. 3, pp. 23–30, 2019.

[14] J. Liu, T. Zhang, and Y. Zhang, "Numerical study on flow-inducednoise for a steam stop-valve using large eddy simulation," *Journal of Marine Science and Application*, vol. 12, no. 3, pp. 351–360, 2013.

[15] S. Sreekala and S. Thirumalini, "Investigation on aerodynamic noise evaluation and attenuation in a globe valve using CFD analysis," *The International Journal of Multiphysics*, vol. 10, no. 1, pp. 43–52, 2016.

[16] J. Li and S. Zhao, "Optimization of valve opening process for the suppression of impulse exhaust noise," *Journal of Sound and Vibration*, vol. 389, no. 2, pp. 24–40, 2017.
[17] X. Xie, W. Zhang, H. Wang et al., "Dynamic adaptive residual network for liver CT image segmentation," *Computers & Electrical Engineering*, vol. 91, Article ID 107024, 2021.
[18] J. Zhang, N. Qi, and J. Jiang, "Effect of cone throttle valve pressure on cavitation noise," *Journal of Engineering*, vol. 2020, no. 7, pp. 275–281, 2020.
[19] S. Li, J. Hou, W. Pan, Z. Wang, and Y. Kang, "Study on aerodynamic noise numerical simulation and characteristics of safety valve based on dipole and quadrupole," *Acoustics Australia*, vol. 48, no. 3, pp. 441–454, 2020.
[20] L. Wei, G. Zhu, J. Qian, Y. Fei, and Z. Jin, "Numerical simulation of flow-induced noise in high pressure reducing valve," *PLoS One*, vol. 10, no. 6, Article ID e0129050, 2015.
[21] S. Rammohan, S. Saseendran, and S. Kumaraswamy, "Effect of multi jets on cavitation performance of globe valves," *Journal of Fluid Science and Technology*, vol. 4, no. 1, pp. 128–137, 2009.
[22] D. Marini and J. R. Corney, "A methodology for near net shape process feasibility assessment," *Production & Manufacturing Research*, vol. 5, no. 1, pp. 390–409, 2017.
[23] X. Xie, X. Pan, W. Zhang, and J. An, "A context hierarchical integrated network for medical image segmentation," *Computers & Electrical Engineering*, vol. 101, Article ID 108029, 2022.
[24] W. Kang, S. H. Lee, S. J. Lee, Y. C. Ha, and S. S. Jung, "Effect of ultrasonic noise generated by pressure control valves on ultrasonic gas flowmeters," *Flow Measurement and Instrumentation*, vol. 60, no. 4, pp. 95–104, 2018.
[25] R. Lah, "Prevent cavitation to minimize control valve damage," *Opflow*, vol. 45, no. 7, pp. 18–20, 2019.
[26] D. Marini and J. R. Corney, "Process selection methodology for near net shape manufacturing," *International Journal of Advanced Manufacturing Technology*, vol. 106, no. 5-6, pp. 1967–1987, 2020.
[27] X. M. Zhou, Z. K. Wang, and Y. F. Zhang, "A simple method for high-precision evaluation of valve flow coefficient by computational fluid dynamics simulation," *Advances in Mechanical Engineering*, vol. 9, no. 7, Article ID 168781401771370, 2017.
[28] J. H. Lee and K. H. Lee, "Prediction of the resistance coefficient in a segment ball valve," *Journal of Mechanical Science and Technology*, vol. 24, no. 1, pp. 185–188, 2010.
[29] G. Ferrarese, G. V. Messa, M. M. A. Rossi, and S. Malavasi, "New method for predicting the incipient cavitation index by means of single-phase computational fluid dynamics model," *Advances in Mechanical Engineering*, vol. 7, no. 3, Article ID 168781401557597, 2015.